Increased Th17-Inducing Activity of CD14$^+$ CD163^{low} Myeloid Cells in Intestinal Lamina Propria of Patients With Crohn's Disease

TAKAYUKI OGINO,[1] JUNICHI NISHIMURA,[1] SOUMIK BARMAN,[2,3] HISAKO KAYAMA,[2,3] SATOSHI UEMATSU,[4] DAISUKE OKUZAKI,[5] HIDEKI OSAWA,[1] NAOTSUGU HARAGUCHI,[1] MAMORU UEMURA,[1] TAISHI HATA,[1] ICHIRO TAKEMASA,[1] TSUNEKAZU MIZUSHIMA,[1] HIROFUMI YAMAMOTO,[1] KIYOSHI TAKEDA,[2,3,6] YUICHIRO DOKI,[1] and MASAKI MORI[1]

[1]Department of Gastroenterological Surgery, [2]Laboratory of Immune Regulation, Graduate School of Medicine, Osaka University, Osaka, Japan; [3]Laboratory of Mucosal Immunology, Immunology Frontier Research Center, Osaka University, Osaka, Japan; [4]Division of Innate Immune Regulation, International Research and Development Center for Mucosal Vaccines, Institute of Medical Science, Tokyo University, Tokyo, Japan; [5]DNA-Chip Developemental Center for Infectious Diseases, Research Institute for Microbial Diseases, Osaka University, Osaka, Japan; and [6]Core Research for Evolutional Science and Technology, Japan Science and Technology Agency, Saitama, Japan

BACKGROUND & AIMS: Abnormal activity of innate immune cells and T-helper (Th) 17 cells has been implicated in the pathogenesis of autoimmune and inflammatory diseases, including Crohn's disease (CD). Intestinal innate immune (myeloid) cells have been found to induce development of Th17 cells in mice, but it is not clear if this occurs in humans or in patients with CD. We investigated whether human intestinal lamina propria cells (LPCs) induce development of Th17 cells and whether these have a role in the pathogenesis of CD. **METHODS:** Normal intestinal mucosa samples were collected from patients with colorectal cancer and noninflamed and inflamed regions of mucosa were collected from patients with CD. LPCs were isolated by enzymatic digestion and analyzed for expression of HLA-DR, lineage markers CD14 and CD163 using flow cytometry. **RESULTS:** Among HLA-DR^{high} Lin$^-$ cells, we identified a subset of CD14$^+$ CD163^{low} cells in intestinal LPCs; this subset expressed Toll-like receptor (*TLR*) *2*, *TLR4*, and *TLR5* mRNAs and produced interleukin (IL)-6, IL-1β, and tumor necrosis factor in response to lipopolysaccharide. In vitro co-culture with naïve T cells revealed that CD14$^+$ CD163^{low} cells induced development of Th17 cells. CD14$^+$ CD163^{low} cells from inflamed regions of mucosa of patients with CD expressed high levels of *IL-6*, *IL-23p19*, and tumor necrosis factor mRNAs, and strongly induced Th17 cells. CD14$^+$ CD163^{low} cells from the noninflamed mucosa of patients with CD also had increased abilities to induce Th17 cells compared with those from normal intestinal mucosa. **CONCLUSIONS: CD14$^+$ CD163^{low} cells in intestinal LPCs from normal intestinal mucosa induce differentiation of naive T cells into Th17 cells; this activity is increased in mucosal samples from patients with CD. These findings show how intestinal myeloid cell types could contribute to pathogenesis of CD and possibly other Th17-associated diseases.**

Keywords: Dendritic Cell; Macrophage; Helper T Cell; Inflammatory Bowel Disease.

Recent studies have suggested that innate immune cells, including macrophages and dendritic cells (DC) of the intestinal mucosa, play important roles in maintaining gut homeostasis by protecting the host from foreign pathogens and by negatively regulating excess immune responses to commensal bacteria and dietary antigens.[1,2] Inappropriate immune reactions to commensal bacteria can lead to development of inflammatory bowel diseases (IBD), such as Crohn's disease (CD) and ulcerative colitis.[3,4] The identification of interleukin (IL)-17–producing Th17 cells offers new insight into the induction and regulation of mucosal immunity, which is linked to IBD pathogenesis.[5–7] Additionally, genome-wide association studies have shown significant associations of CD with Th17-related inflammatory pathways and innate microorganism sensors.[8–13]

Several subsets of murine intestinal innate immune cells have been found to modulate intestinal homeostasis.[14] In the CD11c$^+$ cell subset, CD103$^+$ and CX3CR1$^+$ cells represent nonoverlapping populations with different precursors.[15–17] CD103$^+$ cells uptake luminal antigens in the lamina propria by a unique mechanism, move to the mesenteric lymph nodes (MLN), and activate T cells.[18,19] They can induce expression of gut homing receptors (CCR9 and $\alpha4\beta7$ integrin) on T cells, activate CD8$^+$ T cells, and induce differentiation of Foxp3-expressing regulatory T cells.[20–22] CX3CR1$^+$ cells can be divided into 2 subsets based on CX3CR1 expression level: CX3CR1^{int} and CX3CR1^{high} cells.[15,23] CX3CR1^{int} cells are DCs that induce Th17 cells and migrate into the inflammatory regions,[23–28] and CX3CR1^{high} cells possess anti-inflammatory properties and inhibit T-cell responses.[26,29,30] These findings strongly support the notion that intestinal innate immune cells regulate gut homeostasis.

Compared with murine intestinal innate immune cells, human intestinal cells remain less well characterized. It

Abbreviations used in this paper: CD, Crohn's disease; CDi, inflamed region of CD; CDn, noninflamed region of CD; DC, dendritic cell; IBD, inflammatory bowel disease; IFN, interferon; IL, interleukin; int, intermediate; LPC, lamina propria cell; MLN, mesenteric lymph node; mRNA, messenger RNA; NC, normal colon from colon cancer patients; slan, 6-sulfo LacNAc; TGF, transforming growth factor; Th, T-helper; TLR, Toll-like receptor; TNF, tumor necrosis factor.

© 2013 by the AGA Institute
0016-5085/$36.00
http://dx.doi.org/10.1053/j.gastro.2013.08.049

has been reported that resident intestinal macrophages fail to produce proinflammatory cytokines in response to Toll-like receptor (TLR) ligands, in spite of active phagocytic and bactericidal activities.[31,32] A unique subset of macrophages that express macrophage (CD14, CD33, CD68) and DC (CD205, CD209) markers reportedly contributes to IBD pathogenesis through induction of IL-23–dependent interferon (IFN) gamma responses by T cells, as well as potent antigen-presenting activity.[33,34] Similar to the mouse intestinal CD103$^+$ cells, CD103$^+$ DCs that can induce gut homing receptors have been identified in the human small intestine.[20] However, human intestinal lamina propria cells (LPCs) equivalent to mouse CX3CR1$^+$ cells have not yet been characterized. Most recently, human LPCs have been classified into subsets based on the expressions of CD14, HLA-DR, CD209, CD163, and CD11c.[28] However, functional characterization of these human LPC subsets remains elusive.

In the present study, we show that HLA-DR^{high} Lin$^-$ cells in human intestinal lamina propria comprise 4 subsets that are distinguished by differential expression patterns of CD14, CD11c, and CD163. We further show that HLA-DR^{high} Lin$^-$ CD14$^+$ CD163^{low} cells induce Th17 cell differentiation. CD patients exhibited exceedingly enhanced Th17 immunity induced by HLA-DR^{high} Lin$^-$ CD14$^+$ CD163^{low} cells, even in noninflamed intestine.

Methods

Tissue Samples

Normal intestinal mucosa was obtained from microscopically and macroscopically intact areas in patients with colorectal cancer. Intestinal mucosa was also obtained from surgically resected specimens from patients with CD who were diagnosed based on established clinical, bacteriological, radiologic, and endoscopic criteria. Histopathological analysis showed moderate to severe inflammation in all samples from patients with CD. This study was approved by the Ethical Committee of Osaka University School of Medicine and informed consent for specimen use was obtained from all patients.

Isolation of LPCs

To isolate LPCs, intestinal mucosa was washed in phosphate-buffered saline to remove feces. Then, intestinal mucosa was placed in RPMI 1640 containing 5 mM EDTA and incubated for 10 minutes in a 37°C shaking water bath. After washing in phosphate-buffered saline, the mucosa was cut into small pieces and incubated in RPMI 1640 containing 10% fetal bovine serum, 2 mg/mL collagenase D (Roche, Basel, Switzerland), 1 mg/mL dispase (Invitrogen, Carlsbad, CA), and 15 μg/mL DNase I (Roche) for 60 minutes in a 37°C shaking water bath. The digested tissues were then passed through a 40-μm cell strainer. The isolated cells were washed with RPMI 1640 containing 5 mM EDTA, resuspended in 5 mL 20% Percoll (GE Healthcare Japan, Tokyo, Japan), and then overlaid on 2.5 mL 40% Percoll in a 15-mL tube. Percoll gradient separation was performed by centrifugation at 500*g* for 30 min at 4°C. The LPCs were collected from the interface of the Percoll gradient, then washed twice with phosphate-buffered saline containing 2% fetal bovine serum.

Flow Cytometry

The antibodies for flow cytometry are shown in the Supplementary Material. Flow cytometric analysis was performed using a FACSCantoII flow cytometer (BD Biosciences, San Jose, CA). LPCs were purified using a FACSAriaII system (BD Biosciences), and data were analyzed with FlowJo software (Tree Star, Ashland, OR).

Morphological Analysis

Isolated LPC subsets were spread on glass slides and were air dried. The spread cells were fixed with methanol, stained by May-Grünwald-Giemsa method, and observed with a microscope (BZ-9000; KEYENCE, Itasca, IL).

Microarray Analysis

Total RNA derived from LPCs was reverse transcribed by using an Ovation Pico WTA System V2 (NuGen, San Carlos, CA) and labeled with cyanine-3 using a Genomic DNA Enzymatic Labeling Kit (Agilent Technologies, Santa Clara, CA). The labeled complementary DNA was hybridized to SurePrint G3 Human Gene Expression v2 8x60K Microarray (G4845A) (Agilent Technologies). The data have been deposited in GEO as GSE49066. See the Supplemental Material for more details.

Quantitative Real-Time Reverse Transcription Polymerase Chain Reaction

Total RNA was isolated using the RNeasy Mini kit (Qiagen, Valencia, CA). RNA was reverse-transcribed using Moloney murine leukemia virus reverse transcriptase (Promega, Madison, WI) and random primers (TOYOBO, Osaka, Japan) after treatment with RQ1DNase I (Promega). Quantitative real-time polymerase chain reaction was performed on a Light Cycler 2.0 (Roche) with the TaqMan Universal PCR Master Mix (Applied Biosystems, Carlsbad, CA). Amplification conditions were 95°C for 10 minutes, then 45 cycles of 95°C for 10 seconds, and 60°C for 30 seconds. All data were normalized to the expression of the glyceraldehyde 3-phosphate dehydrogenase gene. The primer sets and probes are shown in Supplementary Table 1.

Cytokine Assay

LPCs were cultured with 1 μg/mL FSL-1 (Invivogen), 1 μg/mL LPS (Sigma, St Louis, MO), or 1 μg/mL flagellin (Invivogen) for 72 hours at 37°C. The culture supernatants were collected and enzyme-linked immunosorbent assay was performed with the Human Th1/Th2 11plex FlowCytomix kit (eBioscience, San Diego, CA).

In Vitro T-Cell Differentiation

Allogeneic naive CD4$^+$ T cells were co-cultured at 37°C with the indicated cells at a ratio of 1:5 in the presence of 10 U/mL IL-2 (Roche), 2 μg/mL anti-CD3 (BD Biosciences), and 5 μg/mL anti-CD28 (BD Biosciences). After 5 days, cells were analyzed by fluorescence-activated cell sorting. In cytokine blocking experiments, cells were cultured in the presence of 2.5 μg/mL anti–transforming growth factor (TGF)–β, 2.5 μg/mL

anti–IL-1β, 2.5 μg/mL anti–IL-6, or 0.5 μg/mL anti–IL-23 (R&D Systems, Minneapolis, MN).

Statistical Analysis

Differences between the control and experimental groups were evaluated using the Student's t test. Statistical analyses were performed using JMP version 9.02 (SAS Institute, Cary, NC). P values $< .01$ were considered statistically significant.

Results

Phenotypic Characterization of Human Colonic LPC Subsets

We used a combination of surface markers to characterize LPC subsets in noninvaded colonic tissue samples from colorectal cancer patients. After LPC isolation from colonic tissues, single-cell suspensions were analyzed for expression of lineage markers (CD3, CD19, CD20, and CD56), HLA-DR, CD14, CD11c, and CD163 (Figure 1*A*). To characterize LPCs that were involved in mediating T-cell differentiation and activation, we focused on HLA-DR^{high} cells. HLA-DR^{high} Lin$^-$ cells comprised 3.7%–5.1% of total LPCs, and were divided into 3 subsets: CD14$^-$ CD11c^{low}, CD14$^-$ CD11c^{high}, and CD14$^+$ CD11c$^+$ cells. CD14$^-$ CD11c^{low} and CD14$^-$ CD11c^{high} cells each did not express CD163 (data not shown), and CD14$^+$ CD11c$^+$ cells were further subdivided into 2 populations: CD163^{low} CD14$^+$ CD11c$^+$ and CD163^{high} CD14$^+$ CD11c$^+$ cells; hereafter, these cells are designated CD14$^+$ CD163^{low} and CD14$^+$ CD163^{high} cells, respectively. In total, human colonic HLA-DR^{high} Lin$^-$ cells comprised 4 subsets: CD14$^+$ CD163^{low} (24.7% $\pm$ 8.2% of all HLA-DR^{high} Lin$^-$ cells), CD14$^+$ CD163^{high} (14.7% $\pm$ 4.7%), CD14$^-$ CD11c^{high} (18.8% $\pm$ 7.9%), and CD14$^-$ CD11c^{low} (30.3% $\pm$ 8.9%) cells (Figure 1*B*). CD14$^+$ CD163^{low} and CD14$^+$ CD163^{high} cells showed macrophage-like morphologies with numerous cytoplasmic vacuoles (Figure 1*C*).

We then analyzed whether these populations were present in other tissues (Figure 1*D*). In the small intestinal

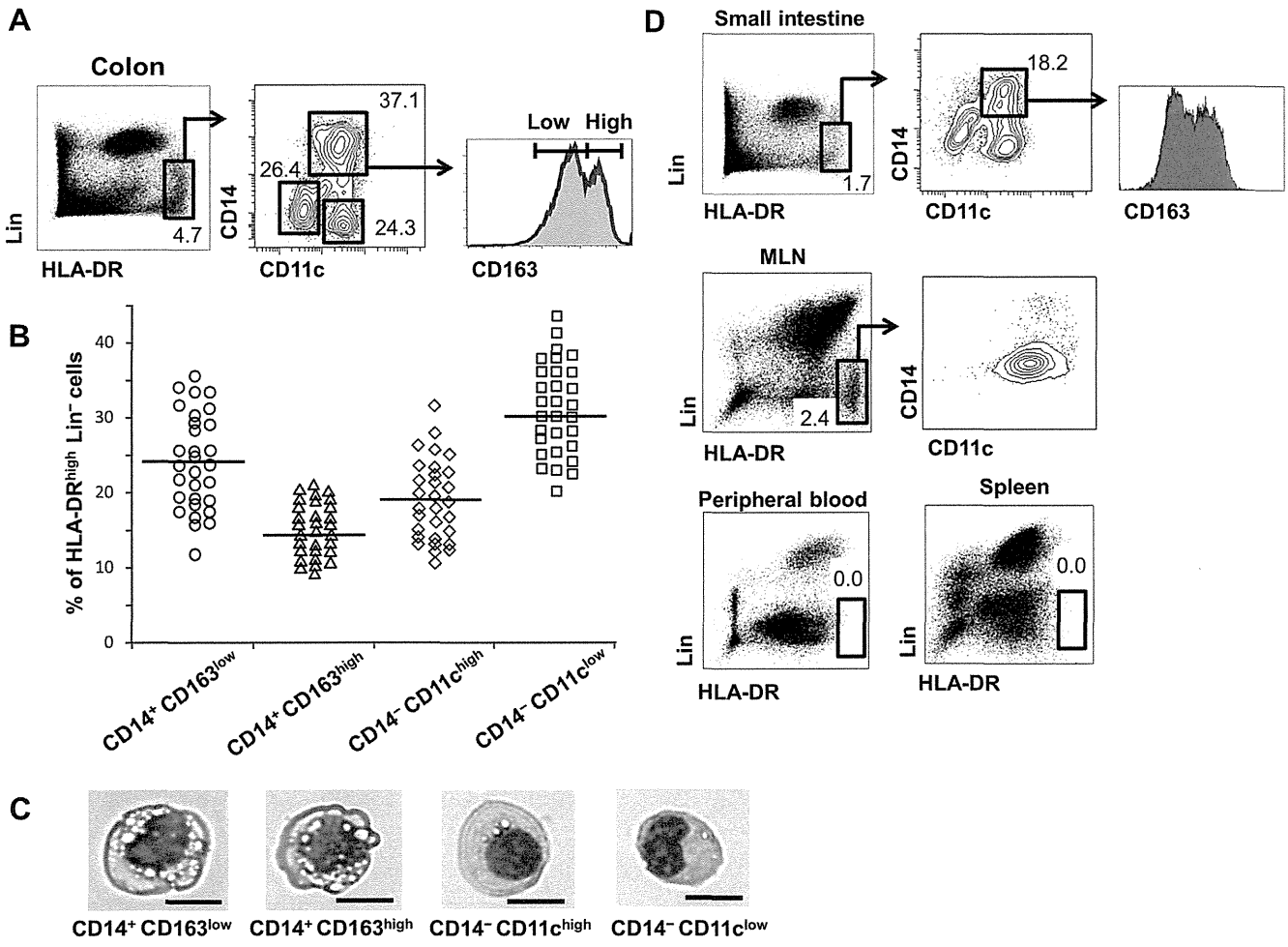

Figure 1. Characterization of LPC subsets. (*A*) Flow cytometry analysis of LPCs from normal intestine of colorectal cancer patients. Live HLA-DR^{high} Lin$^-$ cells were gated and analyzed for expression of CD14 vs CD11c (Lin; CD3, CD19, CD20, CD56). Three populations were defined (CD14$^-$ CD11c$^-$, CD14$^-$ CD11c$^+$, and CD14$^+$ CD11c$^+$), and the CD14$^+$ CD11c$^+$ population was further analyzed for CD163 expression. Representative results of 30 independent experiments are shown. (*B*) Percentages of LPC subsets among HLA-DR^{high} Lin$^-$ cells of 30 patients; *horizontal bars* indicate mean. (*C*) Morphological analysis of LPC subsets by May-Grünwald-Giemsa staining. Scale bars = 10 μm. (*D*) Characterization of cell subsets from human small intestine, MLN, peripheral blood, and spleen. Representative results of 10 independent experiments are shown. *Numbers* indicate the percentage of cells in indicated gates. *Arrows* show gating strategy.

lamina propria, we observed the same 4 populations, albeit with slightly different proportions: $CD14^+$ $CD163^{low}$ (11.7% ± 4.3% of all $HLA\text{-}DR^{high}$ Lin^- cells), $CD14^+$ $CD163^{high}$ (9.9% ± 4.1%), $CD14^-$ $CD11c^{high}$ (35.1% ± 17.2%), and $CD14^-$ $CD11c^{low}$ (33.2% ± 11.1%) cells. In the MLN, we found only small numbers of $CD14^+$ cells and increased numbers of $CD14^-$ $CD11c^{high}$ cells. $HLA\text{-}DR^{high}$ Lin^- cells were not present in peripheral blood and spleen.

Next, we analyzed the surface expressions of several markers on these 4 subsets of human intestinal LPCs (Figure 2). $CD14^+$ $CD163^{low}$ and $CD14^+$ $CD163^{high}$ cells expressed several macrophage and DC markers, including molecules expressed on macrophages (CD16 and CD64), on DCs (CD1c, CD141, CD209, and 6-sulfo LacNAc [slan]), on both macrophages and DCs (CD11b, CD172a, and CD206), and on mature DCs (CD80, CD83, and CD86). These 2 cell subpopulations showed almost the same expression patterns for all examined surface molecules, indicating that CD163 is a unique marker that can distinguish $CD14^+$ cells subpopulations. $CD14^-$ $CD11c^{high}$ cells exhibited high expression of CD1c and CD172a as well as moderate expression of DC maturation markers, but were still heterogeneous because these cells included $CD103^+$ and $CD103^-$ populations. $CD14^-$ $CD11c^{low}$ cells were also heterogeneous, including $CD141^{high}$ and $CD141^-$ populations.

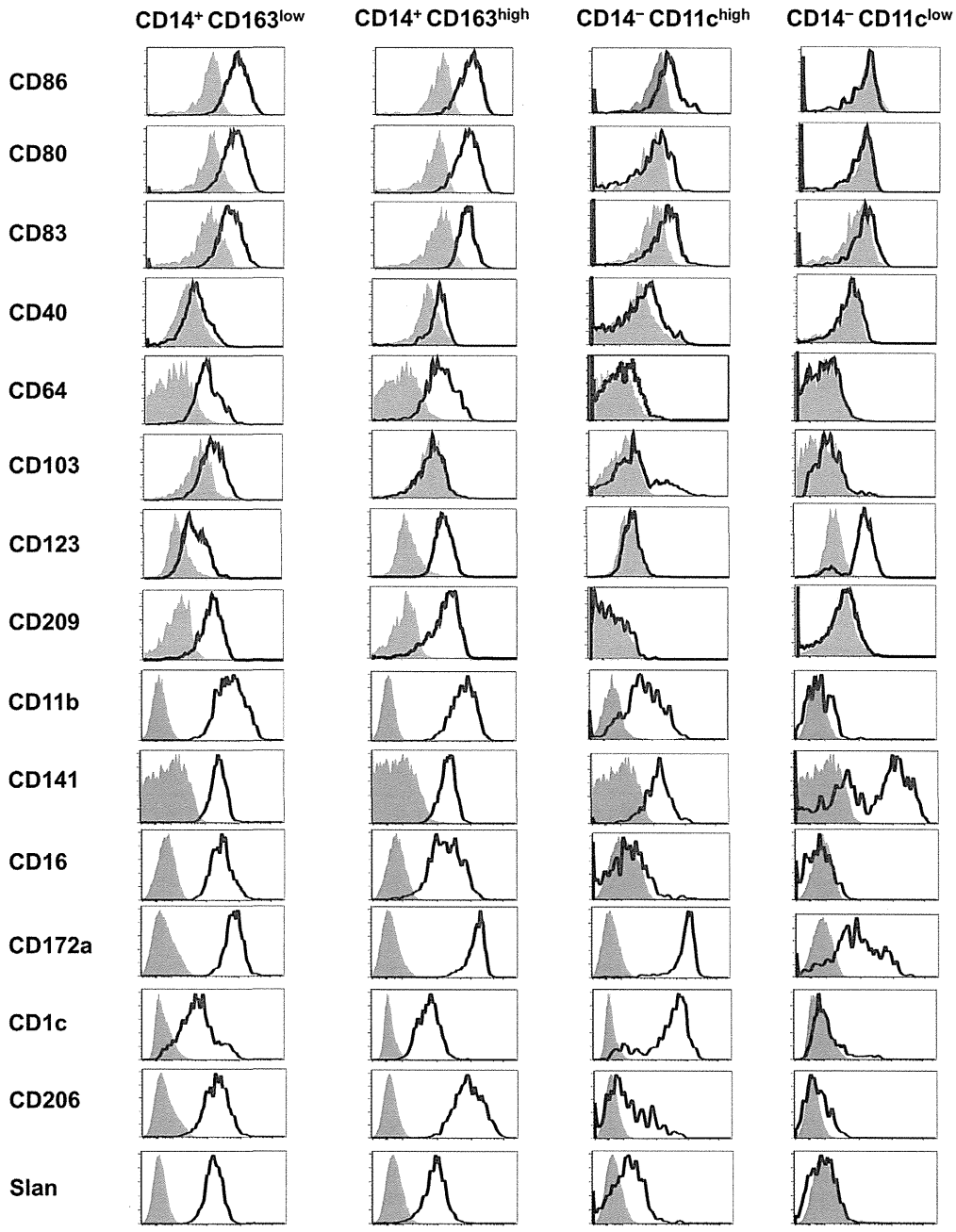

Figure 2. Phenotypic analysis of LPC subsets. Flow cytometry for surface expressions of CD86, CD80, CD83, CD40, CD64, CD103, CD123, CD209, CD11b, CD141, CD16, CD172a, CD1c, CD206, and slan in LPC subsets. The histogram shows the profiles of the indicated antibody staining, and the *shaded* histogram shows staining with isotype control. Representative results of 5–11 independent experiments are shown.

Gene Expression Features of LPC Subsets

We performed microarray analysis to compare gene expression profiles among these subsets purified from normal colon of 10 colon cancer patients. To assess the reliability of the microarray analysis, we compared expression of mRNAs encoding glyceraldehyde 3-phosphate dehydrogenase, CD163, CD14, and CD11c across LPC subsets analyzed (Supplementary Figure 1). We found that mRNA expression of these genes correlated with the surface phenotype of each subset. Hierarchical clustering of about 15,000 protein-coding genes with >2-fold change in expression in at least 1 of the 6 pairwise comparisons showed that $CD14^+$ $CD163^{low}$ cells were more closely related to $CD14^+$ $CD163^{high}$ cells than to other subsets (Figure 3*A*). When we selected genes corresponding to the DC-related and monocyte/macrophage-related biological processes (antigen processing and presentation [GO 0019882], phagocytosis [GO 0006909], monocyte differentiation [GO 0030224], or macrophage differentiation [GO 0030225]), the transcriptomic pathways of $CD14^+$ $CD163^{low}$ cells were found to be similar to those of $CD14^+$ $CD163^{high}$ cells. However, when focusing on inflammatory response to antigenic stimulus (GO 0002437), $CD14^+$ $CD163^{low}$ cells were close to $CD14^-$ $CD11c^{high}$ cells (Figure 3*B* and Supplementary Table 2). To gain more insight into the nature of LPC subsets, we analyzed expression of transcription factors and growth factor receptor, which are involved in function and development of DCs and macrophages (Supplementary Figure 2). Expression of mRNAs encoding *MAFB* and *CSFR1* (involved in macrophage differentiation) was high in $CD14^+$ $CD163^{low}$ and $CD14^+$ $CD163^{high}$ cells. $CD14^-$ $CD11c^{high}$ cells expressed the highest level of mRNAs encoding *IRF4* and *FLT3*, which are both involved in the

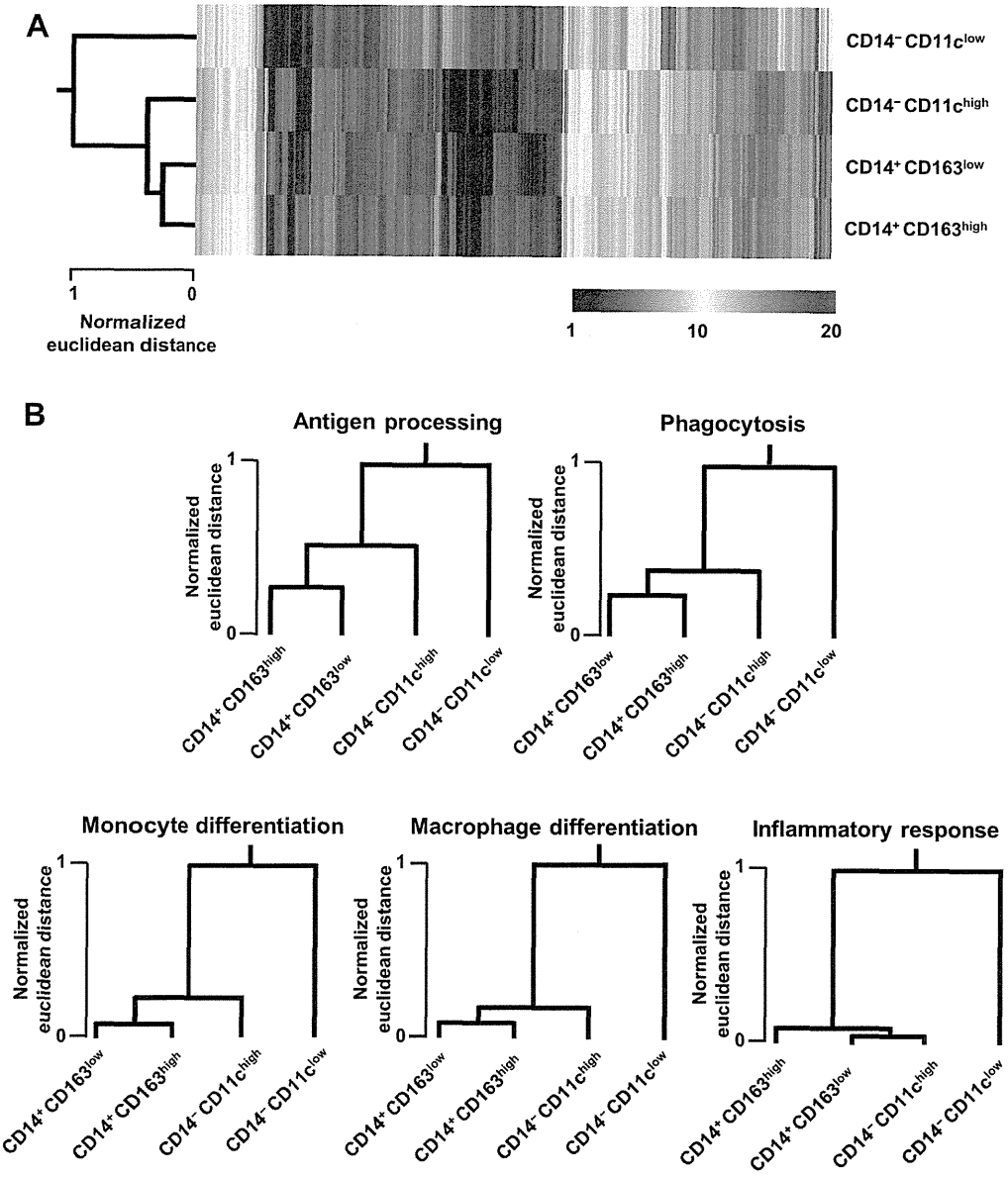

Figure 3. Gene expression profiles of LPC subsets. (*A*) Hierarchical clustering and heat map of LPC subsets was generated from about 15,000 protein-coding genes called detected in at least a subset, with >2-fold change in expression in at least 1 of the 6 possible pairwise comparisons. Euclidian distances are divided by the maximum to scale from 0 to 1. (*B*) Hierarchical clustering using sets of differentially expressed genes corresponding to the Gene Ontology biological functions of antigen processing and presentation (203 genes), phagocytosis (66 genes), monocyte differentiation (16 genes), macrophage differentiation (13 genes), or inflammatory response to antigenic stimulus (15 genes). Clustered heat maps were produced by using Euclidean distance. Euclidian distances are divided by the maximum to scale from 0 to 1.

DC differentiation process. CD14$^+$ CD163^{low} cells showed higher levels of *IRF4* and *FLT3* expression than CD14$^+$ CD163^{high} cells. Taken together, these results suggest that CD14$^+$ CD163^{low} cells are closely related to CD14$^+$ CD163^{high} cells and that the developmental pathway of CD14$^+$ CD163^{low} cells have characteristics of both DC and macrophage development.

We next determined the *TLR* mRNA expression of these 4 subsets by quantitative real-time reverse transcription polymerase chain reaction (Figure 4*A*). CD14$^+$ CD163^{low} cells expressed *TLR2* and *TLR4*, CD14$^+$ CD163^{low}, and CD14$^+$ CD163^{high} cells expressed *TLR5*, and CD14$^-$ CD11c^{high} cells expressed *TLR9*. CD14$^-$ CD11c^{low} cells did not express any *TLR*. We also examined the gene expressions of several inflammatory and anti-inflammatory mediators (Figure 4*B*). CD14$^+$ CD163^{low} cells exhibited the highest expressions of *IL-6* and *IL-23p19*. CD14$^+$ CD163^{high} cells uniquely expressed several anti-inflammatory markers, including *IL-10, HMOX1,* and *TGFB*. CD14$^-$ CD11c^{high} cells expressed the highest level of *IFNG* among the 4 subsets. *IL-12p35* expression was observed only in CD14$^-$ CD11c^{low} cells. Overall, the 4 subsets of intestinal LPCs showed differential expression patterns of inflammatory genes, and the CD14$^+$

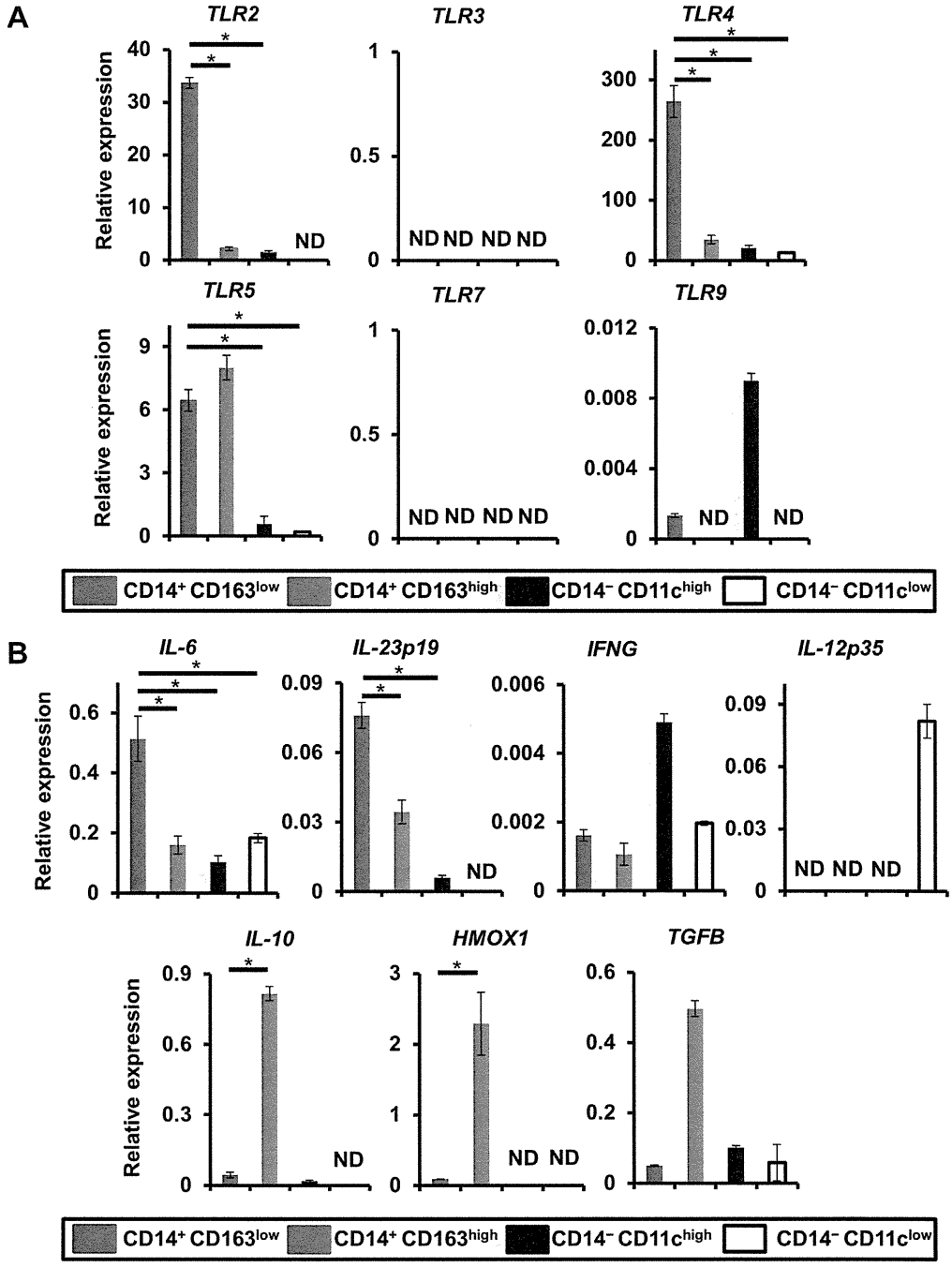

Figure 4. Various mRNA expression of LPC subsets. (*A*) Expression of *TLR2, TLR3, TLR4, TLR5, TLR7,* and *TLR9* in LPC subsets. (*B*) Expression of *IL-6, IL-23p19, IFNG, IL-12p35, IL-10, HMOX1,* and *TGFB* in LPC subsets. Results are mean ± SD from 5 independent experiments. ND, not detected. *$P < .01$.

$CD163^{high}$ cells were unique in their expression of anti-inflammatory genes.

Cytokine Production of LPC Subsets in Response to TLR Stimulation

To analyze the functions of these 4 subsets, we used enzyme-linked immunosorbent assay to assess their cytokine productions in response to TLR stimulation (Figure 5). Based on the *TLR* mRNA expression patterns, we used the TLR2 ligand FSL-1, the TLR4 ligand LPS, and the TLR5 ligand flagellin. High production of inflammatory cytokines, such as IL-6, IL-1β, and TNF-α, was observed in the $CD14^+$ $CD163^{low}$ cells, even without stimulation. $CD14^+$ $CD163^{low}$ cells produced increased amounts of IL-6, IL-1β, and TNF-α in response to LPS, but not in response to FSL-1 or flagellin. $CD14^+$ $CD163^{high}$ cells showed constitutive high production of IL-10, and $CD14^-$ $CD11c^{low}$ cells produced IL-12p70 in response to LPS and flagellin. These findings revealed differential patterns of cytokine production in the 4 LPC subsets, with the $CD14^+$ $CD163^{low}$ cells exhibiting LPS-induced inflammatory responses.

Induction of Th17 Cells by $CD14^+$ $CD163^{low}$ Cells

We next used the allogeneic mixed lymphocyte reaction technique to examine whether the 4 subsets induced Th1 or Th17 cell differentiation. After 5 days of co-culture, the IFN gamma and IL-17 productions of $CD4^+$ T cells were analyzed by intracellular cytokine staining (Figure 6*A*). We used monocyte-derived DCs as a control, which induced IFN-gamma–producing $CD4^+$ T cells (Th1 cells: 15.22% ± 7.19%), but not IL-17–producing $CD4^+$ T cells (Th17 cells: 0%). Naïve $CD4^+$ T cells co-cultured with $CD14^+$ $CD163^{low}$ cells produced high amounts of IL-17 (0.52% ± 0.17%) compared with those co-cultured with other subsets (Figure 6*B*), indicating that $CD14^+$ $CD163^{low}$ cells possess a high capacity

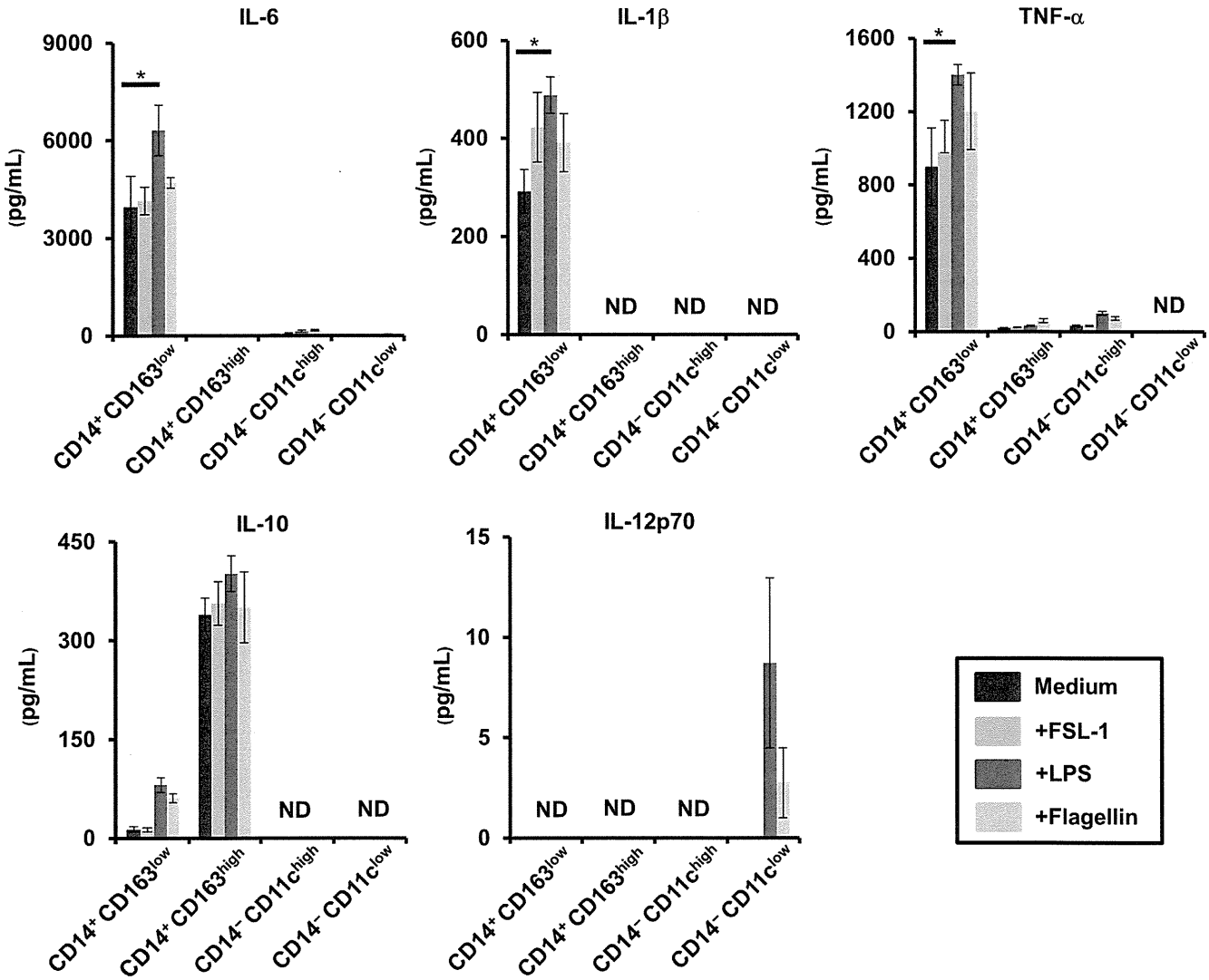

Figure 5. Cytokine production of LPC subsets. LPC subsets were analyzed for productions of IL-6, IL-1β TNF-α, IL-10, and IL-12p70 in response to FSL-1, LPS, or flagellin by enzyme-linked immunosorbent assay. Results are mean ± SD from 5 independent experiments. ND, not detected. *$P < .01$.

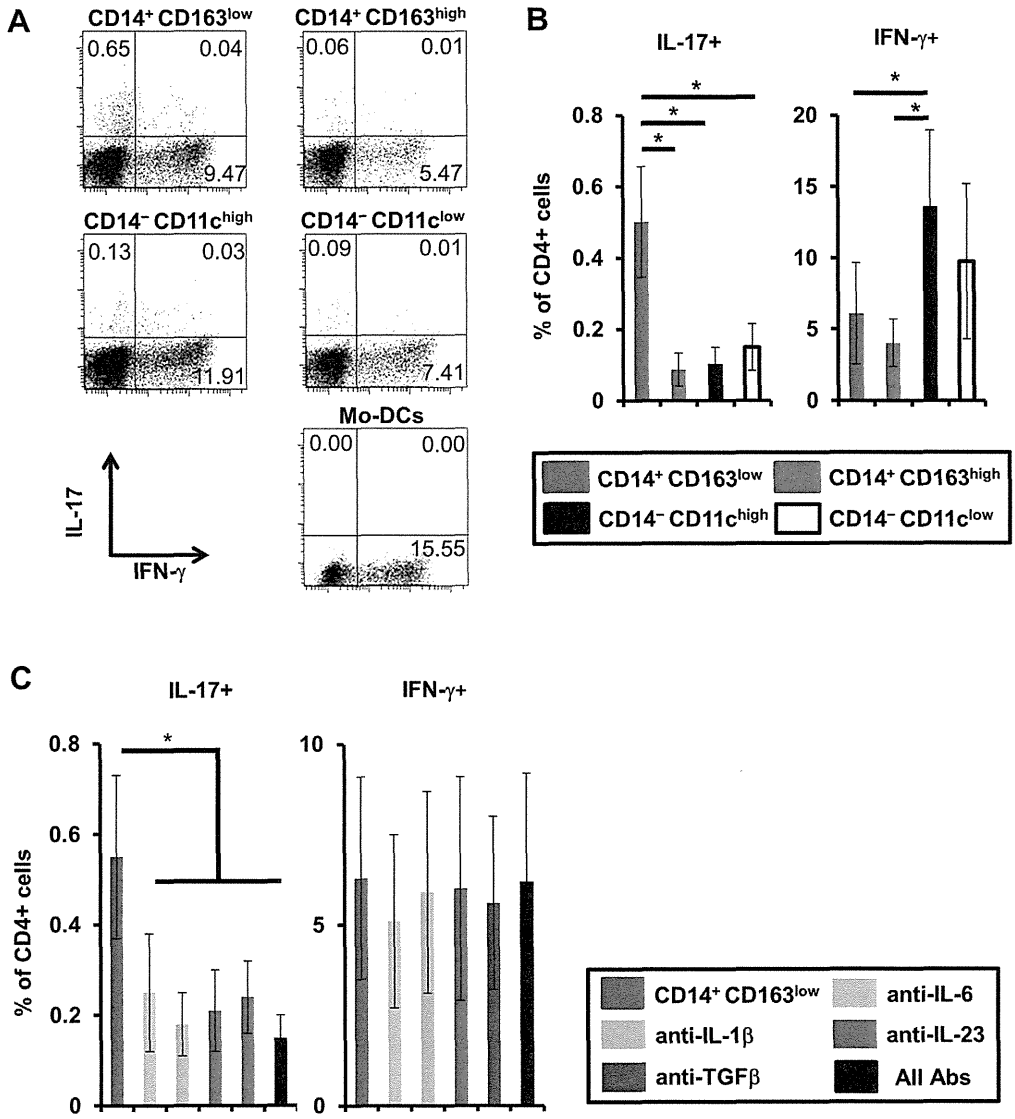

Figure 6. Functional properties of T-cell differentiation in LPC subsets. (*A*) Intracellular cytokine staining and flow cytometry performed to evaluate IFN gamma and IL-17 expression by naive T cells after 5 days of co-culture with allogeneic LPC subsets. Co-culture with monocyte-derived DCs was used as a control. Representative results of 8–14 independent experiments are shown. (*B*) Percentages of IL-17–producing cells and IFN gamma–producing cells among the $CD4^+$ cells after co-culture are shown. Results are mean ± SD from 7 independent experiments. $^*P < .01$. (*C*) Intracellular cytokine (IL-17 and IFN gamma) staining of naive T cells after co-culture with allogeneic $CD14^+$ $CD163^{low}$ subsets in the presence or absence of the indicated blocking antibodies. Percentages of IL-17–producing cells and IFN gamma–producing cells among the $CD4^+$ cells are shown. Results are mean ± SD from 5 independent experiments. $^*P < .01$.

to induce Th17 cells. Naïve $CD4^+$ T cells co-cultured with $CD14^-$ $CD11c^{high}$ cells produced high amounts of IFN gamma (13.78% ± 7.02%), indicating that $CD14^-$ $CD11c^{high}$ cells are DCs with a strong ability to induce Th1 cells. $CD14^-$ $CD11c^{low}$ cells induced moderate levels of Th1 cells (9.81% ± 6.75%) and very few, if any, Th17 cells (0.15% ± 0.06%). The $CD14^+$ $CD163^{high}$ cells showed the lowest ability to induce both Th1 and Th17 cells (4.07% ± 1.61% and 0.08% ± 0.04%, respectively). Overall, the 4 LPC subsets had differential activities for inducing Th1 and Th17 cells, with the $CD14^+$ $CD163^{low}$ cells highly inducing Th17 cells.

To analyze the impacts of IL-6, IL-1β, IL-23, and TGF-β on $CD14^+$ $CD163^{low}$ cell-dependent induction of Th17 cells, we blocked the effect of these cytokines using neutralizing antibodies. Th17 cell differentiation by $CD14^+$ $CD163^{low}$ cells was severely impaired in the presence of the blocking antibodies, and Th1 cell differentiation was not affected (Figure 6*C*).

Functional Analysis of $CD14^+$ $CD163^{low}$ Cells in CD

Because $CD14^+$ $CD163^{low}$ cells facilitated Th17 cell differentiation, we next analyzed these cells in CD patients. Among HLA-DR^{high} Lin^- cells, $CD14^+$ $CD163^{low}$ cells were observed almost equally in the noninflamed region of CD (CDn; 28.1% ± 7.1%) and the inflamed region of CD (CDi; 27.2% ± 7.8%) compared with normal colon from colon cancer patients (NC; 25.5 ± 9.4%) (Figure 7*A* and *B*). We also compared the cytokine gene expression of $CD14^+$ $CD163^{low}$ cells between NC, CDn, and CDi. $CD14^+$ $CD163^{low}$ cells in CDi expressed the highest levels of proinflammatory genes, such as *IL-6*, *IL-23p19*, *TNF*, and *IL-12p35*, as well as anti-inflammatory genes, such as *IL-10* and *TGFB*. $CD14^+$ $CD163^{low}$ cells in CDn also expressed higher *IL-6*, *IL-23p19*, and *TNF* and lower *IL-10* compared with those in NC. *TGFB* expression did not differ between $CD14^+$ $CD163^{low}$ cells in NC and CDn (Figure 7*C*). We next compared the abilities of

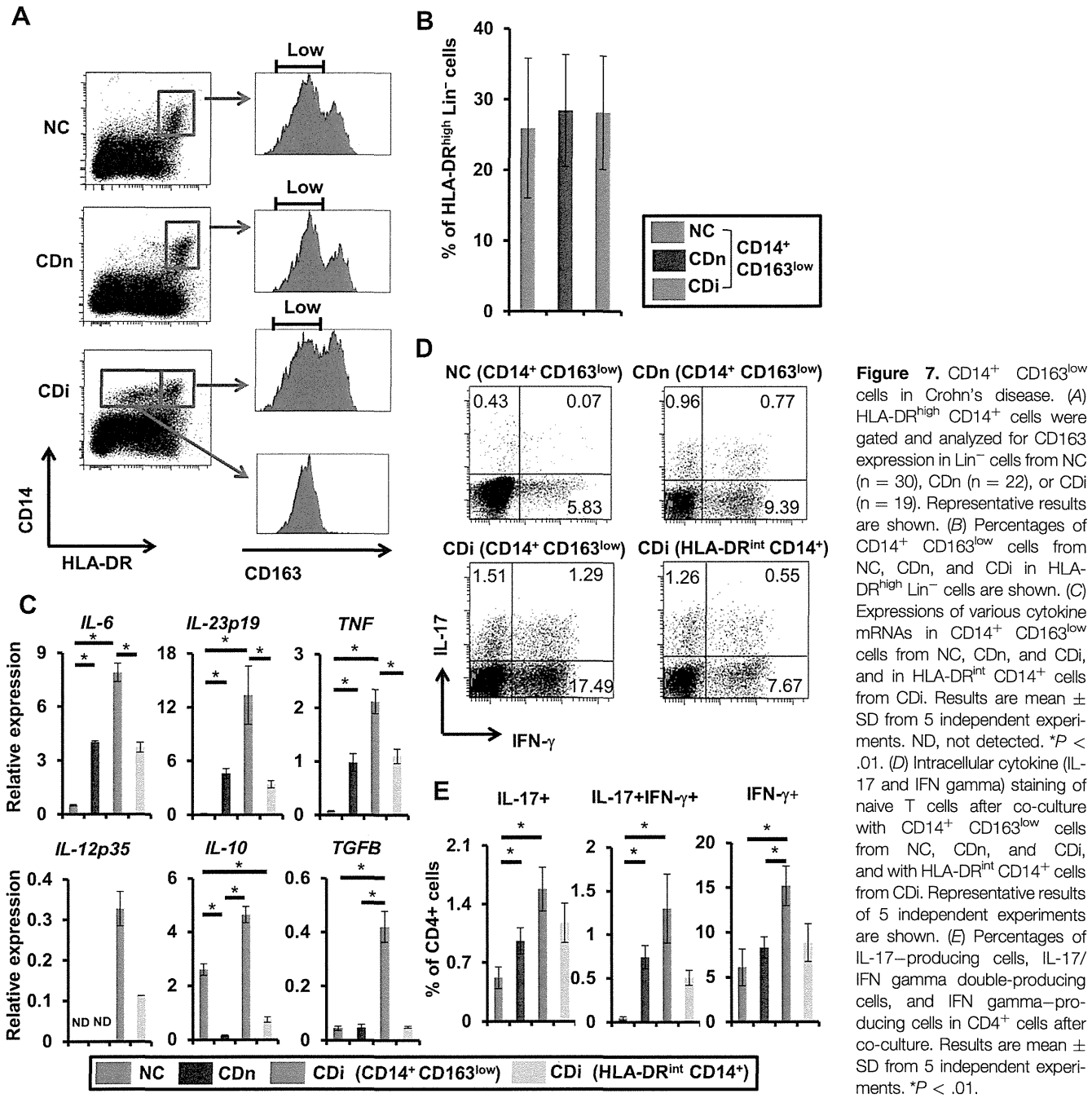

Figure 7. $CD14^+$ $CD163^{low}$ cells in Crohn's disease. (*A*) HLA-DR^{high} $CD14^+$ cells were gated and analyzed for CD163 expression in Lin^- cells from NC (n = 30), CDn (n = 22), or CDi (n = 19). Representative results are shown. (*B*) Percentages of $CD14^+$ $CD163^{low}$ cells from NC, CDn, and CDi in HLA-DR^{high} Lin^- cells are shown. (*C*) Expressions of various cytokine mRNAs in $CD14^+$ $CD163^{low}$ cells from NC, CDn, and CDi, and in HLA-DR^{int} $CD14^+$ cells from CDi. Results are mean ± SD from 5 independent experiments. ND, not detected. *$P <$ .01. (*D*) Intracellular cytokine (IL-17 and IFN gamma) staining of naive T cells after co-culture with $CD14^+$ $CD163^{low}$ cells from NC, CDn, and CDi, and with HLA-DR^{int} $CD14^+$ cells from CDi. Representative results of 5 independent experiments are shown. (*E*) Percentages of IL-17–producing cells, IL-17/IFN gamma double-producing cells, and IFN gamma–producing cells in $CD4^+$ cells after co-culture. Results are mean ± SD from 5 independent experiments. *$P <$ .01.

$CD14^+$ $CD163^{low}$ cells to induce Th1 and Th17 cell differentiation in NC, CDn, and CDi. As mentioned, $CD14^+$ $CD163^{low}$ cells in NC induced approximately 0.5% Th17 cells and few IFN gamma/IL-17 double-producing $CD4^+$ T cells (Th1/17 cells: 0.03% ± 0.01%) (Figure 7*D*). Compared with those in NC, $CD14^+$ $CD163^{low}$ cells in CDn induced similar numbers of Th1 cells (8.31% ± 1.18%), but larger numbers of Th17 (0.96% ± 0.16%) and Th1/17 cells (0.74% ± 0.13%). $CD14^+$ $CD163^{low}$ cells in CDi induced the largest numbers of Th17 cells (1.59% ± 0.26%), Th1/17 cells (1.3% ± 0.39%), and Th1 cells (15.23% ± 2.21%) (Figure 7*D* and *E*).

Interestingly, we found a unique population of HLA-DR intermediate (int) $CD14^+$ cells in CDi. This subset had expression patterns of surface molecules examined similar to $CD14^+$ $CD163^{low}$ cells (Supplementary Figure 3) and high expressions of *IL-6*, *IL-23p19*, and *TNF*, although these levels were lower than those of $CD14^+$ $CD163^{low}$ cells in CDi; these cells also exhibited low *IL-10* expression compared with those in NC (Figure 7*C*). HLA-DR^{int} $CD14^+$ cells induced high levels of Th17 cells (1.18% ± 0.24%) and Th1/17 cells (0.51% ± 0.09%), and moderate levels of Th1 cells (8.83% ± 2.1%) (Figure 7*D* and *E*).

Overall, we found that CD14$^+$ CD163^{low} cells in CDn exhibited high inflammatory cytokine production and strongly induced Th17 cells, and that this ability was further enhanced in CD14$^+$ CD163^{low} cells in CDi. In addition, a unique subset of HLA-DR^{int} CD14$^+$ cells in CDi showed strong ability to produce inflammatory cytokines and to induce Th17 cells.

Discussion

In this study, we characterized differential functions of 4 LPC subsets in the human colon. Within the HLA-DR^{high} Lin$^-$ population, CD14$^+$ CD163^{low} cells mediated Th17 cell differentiation. In CD patients, this subset had strong capacities for cytokine production and Th17 cell induction. It was recently reported that the CD14^{high} population in human ileal mucosa includes HLA-DR^{low} CD209^{low} CD163^{low}, HLA-DR^{high} CD209^{low} CD163^{low}, and HLA-DR^{high} CD209^{high} CD163^{high} cells.[28] In terms of the surface molecule expression patterns in these subsets, HLA-DR^{high} CD209^{low} CD163^{low} cells and HLA-DR^{high} CD209^{high} CD163^{high} cells in that report correspond approximately to the CD14$^+$ CD163^{low} cells and CD14$^+$ CD163^{high} cells, respectively, in the present study.

In mice, subsets of intestinal myeloid cells are already well characterized and are distinguished using combinations of surface markers, such as CD11b, CD11c, CD103, or CX3CR1.[16,21,24,29,35] In contrast, the appropriate surface markers for distinguishing myeloid cell subsets in humans remain unknown. In particular, CX3CR1 expression was hardly detected in human intestinal LPCs (unpublished results). In the present study, we found that LPCs in the HLA-DR^{high} Lin$^-$ population could be divided into CD14$^+$ CD163^{low}, CD14$^+$ CD163^{high}, CD14$^-$ CD11c^{high}, and CD14$^-$ CD11c^{low} subsets.

Mouse intestinal subpopulations, such as CX3CR1^{int} and CX3CR1^{high} cells, are present selectively in the intestine, not in MLN and spleen, under steady state.[25,29,36] Mouse CX3CR1^{int} cells, possessing macrophage-like and DC-like activities, highly express CD11c, major histocompatibility complex class II, and the co-stimulatory molecules CD86 and CD80. Consistent with murine CX3CR1^{int} cell expression of both macrophage (F4/80) and DC (DEC205) markers,[29,37,38] here we found that CD14$^+$ CD163^{low} cells expressed both macrophage- and DC-related markers. Gene expression profile analysis also indicates that CD14$^+$ CD163^{low} cells express genes that mediate macrophage- and DC-related functions. In addition, CD14$^+$ CD163^{low} cells exhibited macrophage-like morphology, like the case in intestinal CX3CR1$^+$ cells in mice.[17,28] These findings suggest that human CD14$^+$ CD163^{low} cells might be equivalent to CX3CR1^{int} cells in mice, which are derived from blood monocytes. CD14$^+$ CD163^{low} cells are monocyte-like lineage of cells that gain an ability of DC-related functions after migrating to the intestine. Similarly, a previous study suggests that CD14^{high} macrophages in normal and CD ileum are similar to CX3CR1^{int} cells in mice.[28] We found that CD14$^+$ CD163^{low} cells produced IL-1β, IL-6, TNF-α, and IL-23p19, as well as the anti-inflammatory cytokine IL-10. A recent study in mice suggests that CX3CR1^{int} cells produce not only IL-6 and TNF-α, but also low levels of IL-10.[23] In terms of cytokine production patterns, CD14$^+$ CD163^{low} cells in humans are similar to CX3CR1^{int} cells in mice, as found in the phenotypic analyses mentioned previously, further suggesting that CD14$^+$ CD163^{low} cells are a human counterpart to mouse CX3CR1^{int} cells.

There have been several reports analyzing human DC subsets. CD1c$^+$ cells in the intestinal lamina propria express higher levels of activation markers (CD40, CD83, CD86, HLA-DR) than those in blood and produce IL-23 at steady state.[39] The present study indicates that these CD1c$^+$ LPCs are further subdivided into CD14$^+$ CD163^{low}, CD14$^+$ CD163^{high} and CD14$^-$ CD11c^{high} cells, and that a main producer of IL-23 is CD14$^+$ CD163^{low} cells. Lung CD1c$^+$ DCs within the CD14$^-$ CD11c$^+$ population activate CD8$^+$ T cells with induction of CD103 expression via TGF-β.[40] Given the similar expression pattern of surface molecules, the lung CD1c$^+$ CD14$^-$ CD11c$^+$ DCs might correspond to the CD14$^-$ CD11c^{high} subset in the present study. CD141^{high} DCs, a functional homolog of mouse CD103$^+$ DCs, synthesize TNF-α, but not IL-12p70, in response to TLR3 stimulation.[41] CD141^{high} cells are present within the CD14$^-$ CD11c^{low} population, which produces IL-12p70 in response to LPS in the present study. In this regard, CD141$^-$ population within the CD14$^-$ CD11c^{low} population might be a IL-12p70 producer. Slan DCs expressing 6-sulfo LacNAc drive Th17/Th1 cell differentiation with production of IL-1β, IL-23, IL-12, and IL-6 in psoriasis patients.[42] The slan DCs do not express CD14 and CD163. CD14$^+$ CD163^{low} cells expressed 6-sulfo LacNAc, but had no production of IL-12p70. Given the differential profiles of surface marker expression and cytokine production, CD14$^+$ CD163^{low} cells are considered to be a distinct population from slan DCs observed in psoriasis patients.

Th17 cell-associated pro-inflammatory cytokines, such as IL-17 and IL-23, play key roles in several mouse autoimmune disease models and are thought to be involved in the pathogenesis of human immune disorders.[43-47] Several reports have identified innate immune cells driving Th17 differentiation. In mice, CX3CR1^{int} cells in the intestinal LP induce Th17 cells,[24,25] and TLR5$^+$ lamina propria DCs induce Th17 cell differentiation.[35] IRF4–dependent CD11b$^+$ DCs play a key role on Th17 induction.[48,49] Human ovarian tumor cells and tumor-associated antigen-presenting cells reportedly mediate Th17 cell generation at tumor sites.[50] Additionally, a human Th17-inducing inflammatory DC subset derived from blood monocytes was recently identified in synovial fluid of rheumatoid arthritis patients and inflammatory tumor ascites.[51] Human DCs inducing Th17 cell differentiation in the inflammatory condition have been identified; however, it remains unclear which human intestinal

LPC subsets are responsible for Th17 induction at steady state. In the present study, we showed that $CD14^+$ $CD163^{low}$ cells secreted IL-6 and IL-1β and differentiated naïve T cells into Th17 cells. $CD14^+$ $CD163^{low}$ cells are the main DCs that induce Th17-mediated immunity in the intestine.

Several recent studies have shown that IBD patients exhibit massive infiltration of Th17 cells in inflamed gastrointestinal mucosa, as well as increased serum IL-17 levels.[52,53] Polymorphisms in the gene encoding the IL-23 receptor are associated with CD.[8] In CD patients, TREM-1^+ macrophages are reportedly increased in intestinal mucosa and contribute to intestinal inflammation.[54] Spontaneous production of IL-1β and TNF-α is observed in $CD172a^+$ $HLA\text{-}DR^+$ cells, which accumulate into MLN and the intestinal mucosa of CD patients.[55] In the present study, we showed that the proportion of $CD14^+$ $CD163^{low}$ cells was not altered between NC and CDn. However, Th17 cell differentiation by $CD14^+$ $CD163^{low}$ cells was significantly higher in CDn than in NC. Abnormal activity of $CD14^+$ $CD163^{low}$ cells is evident, even in the non-inflamed intestine of CD patients. In addition, the $CD14^+$ $CD163^{low}$ cells in CDi had extremely enhanced ability to induce Th17 cells. These results indicated that $CD14^+$ $CD163^{low}$ cells might be involved in the progression of CD via Th17 immunity. Compared with NC and CDn, CDi involved huge numbers of $HLA\text{-}DR^{int}$ $CD14^+$ cells. In this regard, $HLA\text{-}DR^{int}$ $CD14^+$ cells might migrate from the bloodstream to the intestine in inflammatory environments, as has been reported for mouse $Ly6c^{high}$ $CX3CR1^{int}$ monocytes, which migrate into the intestine during intestinal inflammation.[28]

In conclusion, here we have identified $CD14^+$ $CD163^{low}$ cells as a subset that produces IL-6 and IL-1β, and can induce Th17 cells in human intestinal lamina propria. Further characterization of human $CD14^+$ $CD163^{low}$ cells showed them to be the putative equivalents of mouse $CX3CR1^{int}$ cells. Based on *TLR* expression and Th17 immunity, $CD14^+$ $CD163^{low}$ cells might play key roles in CD. Our findings suggest that $CD14^+$ $CD163^{low}$ cells could be a new diagnostic and therapeutic target for CD patients.

Supplementary Material

Note: To access the supplementary material accompanying this article, visit the online version of *Gastroenterology* at www.gastrojournal.org, and at http://dx.doi.org/10.1053/j.gastro.2013.08.049.

References

1. Coombes JL, Powrie F. Dendritic cells in intestinal immune regulation. Nat Rev Immunol 2008;8:435–446.
2. Steinman RM, Hawiger D, Nussenzweig MC. Tolerogenic dendritic cells. Annu Rev Immunol 2003;21:685–711.
3. Strober W, Fuss I, Mannon P. The fundamental basis of inflammatory bowel disease. J Clin Invest 2007;117:514–521.
4. Xavier RJ, Podolsky DK. Unravelling the pathogenesis of inflammatory bowel disease. Nature 2007;448:427–434.
5. Neurath MF. IL-23: a master regulator in Crohn disease. Nat Med 2007;13:26–28.
6. Yen D, Cheung J, Scheerens H, et al. IL-23 is essential for T cell-mediated colitis and promotes inflammation via IL-17 and IL-6. J Clin Invest 2006;116:1310–1316.
7. Kobayashi T, Okamoto S, Hisamatsu T, et al. IL23 differentially regulates the Th1/Th17 balance in ulcerative colitis and Crohn's disease. Gut Microbes 2008;57:1682–1689.
8. Duerr RH, Taylor KD, Brant SR, et al. A genome-wide association study identifies IL23R as an inflammatory bowel disease gene. Science 2006;314:1461–1463.
9. Ogura Y, Bonen DK, Inohara N, et al. A frameshift mutation in NOD2 associated with susceptibility to Crohn's disease. Nature 2001;411:603–606.
10. Hugot JP, Chamaillard M, Zouali H, et al. Association of NOD2 leucine-rich repeat variants with susceptibility to Crohn's disease. Nature 2001;411:599–603.
11. Khor B, Gardet A, Xavier RJ. Genetics and pathogenesis of inflammatory bowel disease. Nature 2011;474:307–317.
12. Barrett JC, Hansoul S, Nicolae DL, et al. Genome-wide association defines more than 30 distinct susceptibility loci for Crohn's disease. Nat Genet 2008;40:955–962.
13. Fisher SA, Tremelling M, Anderson CA, et al. Genetic determinants of ulcerative colitis include the ECM1 locus and five loci implicated in Crohn's disease. Nat Genet 2008;40:710–712.
14. Kayama H, Takeda K. Regulation of intestinal homeostasis by innate and adaptive immunity. Int Immunol 2012;24:673–680.
15. Varol C, Vallon-Eberhard A, Elinav E, et al. Intestinal lamina propria dendritic cell subsets have different origin and functions. Immunity 2009;31:502–512.
16. Schulz O, Jaensson E, Persson EK, et al. Intestinal CD103+, but not CX3CR1+, antigen sampling cells migrate in lymph and serve classical dendritic cell functions. J Exp Med 2009;206:3101–3114.
17. Bogunovic M, Ginhoux F, Helft J, et al. Origin of the lamina propria dendritic cell network. Immunity 2009;31:513–525.
18. Farache J, Koren I, Milo I, et al. Luminal bacteria recruit $CD103^+$ dendritic cells into the intestinal epithelium to sample bacterial antigens for presentation. Immunity 2013;21;38:581–595.
19. McDole JR, Wheeler LW, McDonald KG, et al. Goblet cells deliver luminal antigen to CD103+ dendritic cells in the small intestine. Nature 2012;483:345–349.
20. Jaensson E, Uronen-Hansson H, Pabst O, et al. Small intestinal CD103+ dendritic cells display unique functional properties that are conserved between mice and humans. J Exp Med 2008; 205:2139–2149.
21. Sun CM, Hall JA, Blank RB, et al. Small intestine lamina propria dendritic cells promote de novo generation of Foxp3 T reg cells via retinoic acid. J Exp Med 2007;204:1775–1785.
22. Johansson-Lindbom B, Svensson M, Pabst O, et al. Functional specialization of gut CD103+ dendritic cells in the regulation of tissue-selective T cell homing. J Exp Med 2005;202:1063–1073.
23. Weber B, Saurer L, Schenk M, et al. CX3CR1 defines functionally distinct intestinal mononuclear phagocyte subsets which maintain their respective functions during homeostatic and inflammatory conditions. Eur J Immunol 2011;41:773–779.
24. Denning TL, Wang YC, Patel SR, et al. Lamina propria macrophages and dendritic cells differentially induce regulatory and interleukin 17-producing T cell responses. Nat Immunol 2007;8:1086–1094.
25. **Atarashi K, Nishimura J**, Shima T, et al. ATP drives lamina propria TH17 cell differentiation. Nature 2008;455:808–812.
26. Zigmond E, Varol C, Farache J, et al. Ly6C hi monocytes in the inflamed colon give rise to proinflammatory effector cells and migratory antigen-presenting cells. Immunity 2012;37:1076–1090.
27. Rivollier A, He J, Kole A, et al. Inflammation switches the differentiation program of $Ly6C^{hi}$ monocytes from antiinflammatory macrophages to inflammatory dendritic cells in the colon. J Exp Med 2012; 209:139–155.
28. Bain CC, Scott CL, Uronen-Hansson H, et al. Resident and pro-inflammatory macrophages in the colon represent alternative

context-dependent fates of the same Ly6C^{hi} monocyte precursors. Mucosal Immunol 2013;6:498–510.
29. Kayama H, Ueda Y, Sawa Y, et al. Intestinal CX3C chemokine receptor 1 high (CX3CR1^{high}) myeloid cells prevent T-cell-dependent colitis. Proc Natl Acad Sci U S A 2012;109:5010–5015.
30. Hadis U, Wahl B, Schulz O, et al. Intestinal tolerance requires gut homing and expansion of FoxP3^{+} regulatory T cells in the lamina propria. Immunity 2011;34:237–246.
31. Smythies LE. Human intestinal macrophages display profound inflammatory anergy despite avid phagocytic and bacteriocidal activity. J Clin Invest 2005;115:66–75.
32. Smith PD, Smythies LE, Mosteller-Barnum M, et al. Intestinal macrophages lack CD14 and CD89 and consequently are down-regulated for LPS- and IgA-mediated activities. J Immunol 2001; 164:2651–2656.
33. Kamada N, Hisamatsu T, Okamoto S, et al. Unique CD14 intestinal macrophages contribute to the pathogenesis of Crohn disease via IL-23/IFN-gamma axis. J Clin Invest 2008;118:2269–2280.
34. Kamada N, Hisamatsu T, Honda H, et al. Human CD14+ macrophages in intestinal lamina propria exhibit potent antigen-presenting ability. J Immunol 2009;183:1724–1731.
35. Uematsu S, Fujimoto K, Jang MH, et al. Regulation of humoral and cellular gut immunity by lamina propria dendritic cells expressing Toll-like receptor 5. Nat Immunol 2008;9:769–776.
36. Diehl GE, Longman RS, Zhang JX, et al. Microbiota restricts trafficking of bacteria to mesenteric lymph nodes by CX3CR1^{hi} cells. Nature 2013;494:116–120.
37. Tamoutounour S, Henri S, Lelouard H, et al. CD64 distinguishes macrophages from dendritic cells in the gut and reveals the Th1-inducing role of mesenteric lymph node macrophages during colitis. Eur J Immunol 2012;42:1–17.
38. Niess JH, Adler G. Enteric flora expands gut lamina propria CX3CR1^{+} dendritic cells supporting inflammatory immune responses under normal and inflammatory conditions. J Immunol 2010; 184:2026–2037.
39. Dillon SM, Rogers LM, Howe R, et al. Human intestinal lamina propria CD1c+ dendritic cells display an activated phenotype at steady state and produce IL-23 in response to TLR7/8 stimulation. J Immunol 2010;184:6612–6621.
40. Yu CI, Becker C, Wang Y, et al. Human CD1c+ dendritic cells drive the differentiation of CD103+ CD8+ mucosal effector T cells via the cytokine TGF-beta. Immunity 2013;38:818–830.
41. Haniffa M, Shin A, Bigley V, et al. Human tissues contain CD141hi cross-presenting dendritic cells with functional homology to mouse CD103+ nonlymphoid dendritic cells. Immunity 2012;37:60–73.
42. Hansel A, Gunther C, Ingwersen J, et al. Human slan (6-sulfo LacNAc) dendritic cells are inflammatory dermal dendritic cells in psoriasis and drive strong TH17/TH1 T-cell responses. J Allergy Clin Immunol 2011;127:787–794.
43. Wong CK, Lit LC, Tam LS, et al. Hyperproduction of IL-23 and IL-17 in patients with systemic lupus erythematosus: implications for Th17-mediated inflammation in auto-immunity. Clin Immunol 2008; 127:385–393.
44. Ma HL, Liang S, Li J, et al. IL-22 is required for Th17 cell–mediated pathology in a mouse model of psoriasis-like skin inflammation. J Clin Invest 2008;118:597–607.
45. Komiyama Y, Nakae S, Matsuki T, et al. IL–17 Plays an important role in the development of experimental autoimmune encephalomyelitis. J Immunol 2006;177:566–573.
46. Chan JR, Blumenschein W, Murphy E, et al. IL-23 stimulates epidermal hyperplasia via TNF and IL-20R2-dependent mechanisms with implications for psoriasis pathogenesis. J Exp Med 2006; 203:2577–2587.
47. Kurosawa K, Hirose K, Sano H, et al. Increased Interleukin-17 production in patients with systemic sclerosis. Arthritis Rheum 2000; 43:2455–2463.
48. Schlitzer A, McGovern N, Teo P, et al. IRF4 Transcription factor-dependent CD11b+ dendritic cells in human and mouse control mucosal IL-17 cytokine responses. Immunity 2013;38:970–983.
49. Persson EK, Uronen-Hansson H, Semmrich M, et al. IRF4 transcription-factor dependent CD103+CD11b+ dendritic cells drive mucosal T helper 17 cell differentiation. Immunity 2013; 38:958–969.
50. Miyahara Y, Odunsi K, Chen W, et al. Generation and regulation of human CD4^{+} IL-17-producing T cells in ovarian cancer. Proc Natl Acad Sci U S A 2008;105:15505–15510.
51. Segura E, Touzot M, Bohineust A, et al. Human inflammatory dendritic cells induce th17 cell differentiation. Immunity 2013;38:336–348.
52. Veny M, Esteller M, Ricart E, et al. Late Crohn's disease patients present an increase in peripheral Th17 cells and cytokine production compared with early patients. Aliment Pharmacol Ther 2010; 31:561–572.
53. Fujino S, Andoh A, Bamba S, et al. Increased expression of interleukin 17 in inflammatory bowel disease. Gut 2003;52:65–70.
54. Schenk M, Bouchon A, Seibold F, et al. TREM-1-expressing intestinal macrophages crucially amplify chronic inflammation in experimental colitis and inflammatory bowel diseases. J Clin Invest 2007; 117:3097–3106.
55. Baba N, Van VQ, Wakahara K, et al. CD47 fusion protein targets CD172a+ cells in Crohn's disease and dampens the production of IL-1β and TNF. J Exp Med 2013;210:1251–1263.

Author names in bold designate shared co-first authorship.

Received March 29, 2013. Accepted August 22, 2013.

Reprint requests

Address requests for reprints to: Junichi Nishimura, MD, PhD, Department of Gastroenterological Surgery, Graduate School of Medicine, Osaka University, Yamadaoka 2-2, Suita City, Osaka 565-0871, Japan. e-mail: jnishimura@gesurg.med.osaka-u.ac.jp**; fax: 81(0)6 6879 3259; or Kiyoshi Takeda, MD, PhD, Laboratory of Immune Regulation, Graduate School of Medicine, Osaka University, Yamadaoka 2-2, Suita City, Osaka 565-0871, Japan.**
e-mail: ktakeda@ongene.med.osaka-u.ac.jp**; fax: 81(0)6 6879 3989.**

Conflicts of interest

The authors disclose no conflicts.

Supplementary Material

Antibodies for Flow Cytometry

The following antibodies were used: phycoerythrin (PE)-conjugated anti-CD3 (HIT3a; BD Biosciences), anti-CD19 (SJ25C1; BD Biosciences), anti-CD20 (2H7; BD Biosciences), anti-CD56 (B159; BD Biosciences), fluorescein isothiocyanate–conjugated anti-CD14 (MφP9; BD Biosciences), allophycocyanin-conjugated anti-CD11c (B-ly6; BD Biosciences), PE-Cy7–conjugated anti–HLA-DR (L243; Biolegend, San Diego, CA), peridinin chlorophyll protein complex-Cy5.5-conjugated anti-CD163 (GHI61; Biolegend), fluorescein isothiocyanate–conjugated anti-lineage (BD Biosciences), PE-Cy5–conjugated anti-CD86 (2331; BD Biosciences), anti-CD80 (L307.4; BD Biosciences), anti-CD83 (HB15e; BD Biosciences), anti-CD40 (5C3; BD Biosciences), PE-conjugated anti-CD64 (10.1; BD Biosciences), anti-CD103 (Ber-ACT8; Biolegend), anti-CD123 (7G3; BD Biosciences), anti-CD209 (DCN46; BD Biosciences), anti-CD11b (ICRF44; Biolegend), anti-CD141 (M80; Biolegend), anti-CD16 (3G8; BD Biosciences), anti-CD172a (SE5A5; Biolegend), anti-CD206 (15-2; Biolegend), anti-slan (DD-1; Miltenyi Biotec, Bergisch Gladbach, Germany), Brilliant Violet-conjugated anti-CD1c (L161; Biolegend), peridinin chlorophyll protein complex-Cy5.5-conjugated anti-CD4 (SK3; BD Biosciences), PE-conjugated anti-IL17A (N49-653; BD Biosciences), allophycocyanin-conjugated anti–IL-4 (MP4-25D2; BD Biosciences), and fluorescein isothiocyanate–conjugated anti–IFN-gamma (B27; BD Biosciences).

Intracellular Cytokine Analysis

$CD4^+$ T cells were stimulated for 4 hours in the presence of 5 μM calcium ionosphere (Sigma), 50 ng/mL phorbol myristate acetate (Sigma), and GolgiStop (BD Biosciences). Intracellular cytokine staining was subsequently performed with fixation and permeabilization buffers.

Preparation of Monocyte-Derived DCs

Peripheral $CD14^+$ monocytes were isolated from peripheral blood monocytes using CD14 microbeads (Miltenyi Biotec) following the manufacturer's instructions. For in vitro monocyte-derived DC differentiation, $CD14^+$ monocytes were cultured for 5 days in RPMI 1640 containing 10% fetal bovine serum, with 100 ng/mL recombinant human granulocyte macrophage colony-stimulating factor (Primmune, Kobe, Japan) and 100 U/mL recombinant human IL-4 (Primmune).

Microarray Analysis

Gene expression analysis using SurePrint G3 Human Gene Expression v2 8x60K Microarray (G4845A) (Agilent Technologies) was performed as one color experiments by the Dragon Genomics Center (TaKaRa Bio Inc., Shiga, Japan). Total RNA from $CD163^{high}$ ($CD14^+$ $CD163^{high}$), $CD163^{low}$ ($CD14^+$ $CD163^{low}$), DN ($CD14^-$ $CD11c^{low}$) and CD11c ($CD14^-$ $CD11c^{high}$) cells, which were derived from the sorted HLA-DR^{high} Lin^- LPC subsets in noninvaded colonic tissue samples from individual colorectal cancer patients (n = 10) was extracted using RNeasy kit (Qiagen) following manufacturer's instructions. Twenty nanograms total RNA was reverse transcribed into double strand complementary DNAs by using an Ovation Pico WTA System V2 (NuGen) following manufacturer's protocol. Resulting complementary DNAs were subsequently used for in vitro transcription by DNA polymerase and labeled with cyanine-3 using a Genomic DNA Enzymatic Labeling Kit (Agilent Technologies) according to the manufacturer's protocol. After labeling, the labeled 2 μg of each complementary DNA sample was then hybridized on SurePrint G3 Human Gene Expression v2 8x60K Microarray at 65°C for 17 hours with rotation in the dark. Hybridization was performed using a Gene Expression Hybridization Kit (Agilent Technologies) following the manufacturer's instructions. After washing in GE washing buffer, slides were scanned with an Agilent Microarray Scanner G2505C. Feature extraction software (version 10.10.1.1) was used to convert images into gene expression data. Raw data were imported into GeneSpring GX 11.0 (Agilent Technologies) for database management and quality control. This normalized data without the threshold raw signal and the global normalization algorithm was used for identifying differentially expressed genes. Raw data have been accepted in Gene Expression Omnibus, a public repository for microarray data, aimed at storing Minimum Information About Microarray Experiments Access to data concerning this study is found under Gene Expression Omnibus experiment accession number GSE49066.

Cancer Medicine

Open Access

ORIGINAL RESEARCH

Intraperitoneal injection of in vitro expanded Vγ9Vδ2 T cells together with zoledronate for the treatment of malignant ascites due to gastric cancer

Ikuo Wada[1], Hirokazu Matsushita[2], Shuichi Noji[1], Kazuhiko Mori[1], Hiroharu Yamashita[1], Sachiyo Nomura[1], Nobuyuki Shimizu[1], Yasuyuki Seto[1] & Kazuhiro Kakimi[2]

[1]Department of Gastrointestinal Surgery, The University of Tokyo Hospital, Tokyo, Japan
[2]Department of Immunotherapeutics (Medinet), The University of Tokyo Hospital, Tokyo, Japan

Keywords
Gastric cancer, malignant ascites, peritoneal dissemination, Vγ9Vδ2 T-cell, zoledronate

Correspondence
Kazuhiro Kakimi, Department of Immunotherapeutics, The University of Tokyo Hospital, 7-3-1 Hongo, Bunkyo-Ku, Tokyo 113-8655, Japan.
Tel: 81-35805-3161; Fax: 81-35805-3164;
E-mail: kakimi@m.u-tokyo.ac.jp

Funding Information
This study was supported in part by a Grant-in-Aid for Scientific Research of the Ministry of Education, Culture, Sports, Science and Technology (K. K.).

Received: 17 October 2013; Revised: 28 November 2013; Accepted: 29 November 2013

***Cancer Medicine* 2014; 3(2): 362–375**

doi: 10.1002/cam4.196

Abstract

Malignant ascites caused by peritoneal dissemination of gastric cancer is chemotherapy-resistant and associated with poor prognosis. We conducted a pilot study to evaluate the safety of weekly intraperitoneal injections of in vitro expanded Vγ9Vδ2 T cells together with zoledronate for the treatment of such malignant ascites. Patient peripheral blood mononuclear cells were stimulated with zoledronate (5 μmol/L) and interleukin-2 (1000 IU/mL). After 14 days culture, Vγ9Vδ2 T-cells were harvested and administered intraperitoneally in four weekly infusions. The day before T-cell injection, patients received zoledronate (1 mg) to sensitize their tumor cells to Vγ9Vδ2 T-cell recognition. Seven patients were enrolled in this study. The number of Vγ9Vδ2 T-cells in each injection ranged from 0.6 to 69.8 × 10^8 (median 59.0 × 10^8). There were no severe adverse events related to the therapy. Intraperitoneal injection of Vγ9Vδ2 T cells allows them access to the tumor cells in the peritoneal cavity. The number of tumor cells in the ascites was significantly reduced even after the first round of therapy and remained substantially lower over the course of treatment. IFN-γ was detected in the ascites on treatment. Computed tomography revealed a significant reduction in volume of ascites in two of seven patients. Thus, injection of these antitumor Vγ9Vδ2 T-cells can result in local control of malignant ascites in patients for whom no standard therapy apart from paracentesis is available. Adoptively transferred Vγ9Vδ2 T-cells do indeed recognize tumor cells and exert antitumor effector activity in vivo, when they access to the tumor cells.

Introduction

Human T cells carrying γδ T-cell receptors account for 1–5% of peripheral blood T-cells [1, 2], the majority expressing the Vγ9Vδ2 receptor [3] that recognizes phosphoantigens [4, 5]. Recently, much attention has been paid to Vγ9Vδ2 T-cell-based cancer immunotherapy because these cells can secrete cytokines and exert potent cytotoxicity against a wide range of cancer cells [4]. Direct in vivo activation of Vγ9Vδ2 T cells by nitrogen-containing bisphosphonates (NBPs) in cancer patients [6, 7] as well as adoptive transfer of ex vivo expanded Vγ9Vδ2 T cells have been investigated in several clinical trials [8, 9].

We have established a large-scale ex vivo expansion protocol for Vγ9Vδ2 T cells using zoledronate and interleukin-2 (IL-2) [10, 11]. We found that such cultured T cells retained cytokine secretion capacity and mediated cytotoxicity against a variety of cancer cell lines [10]. On the basis of these findings, we conducted a clinical study in patients with advanced or recurrent non-small cell lung cancer resistant to standard therapy [12, 13]. The adoptive transfer of autologous Vγ9Vδ2 T cells was well-tolerated. Some clinical benefit was observed in some

© 2014 The Authors. *Cancer Medicine* published by John Wiley & Sons Ltd. This is an open access article under the terms of the Creative Commons Attribution License, which permits use, distribution and reproduction in any medium, provided the original work is properly cited.

patients in whom Vγ9Vδ2 T-cells were able to survive and expand, and in whom plasma IFN-γ levels were elevated (but without statistical significance) [13]. However, it remained to be determined whether transferred Vγ9Vδ2 T cells infiltrated into the tumor, recognized tumor cells and exerted antitumor effector functions in vivo. Therefore, we conducted a clinical study of intraperitoneal (i.p.) Vγ9Vδ2 T-cell transfer therapy for the treatment of malignant ascites caused by peritoneal dissemination of gastric cancer.

Peritoneal dissemination is frequently observed in cases of advanced gastric cancer and occurs as a consequence of direct invasion and/or metastasis [14]. The presence of malignant ascites is a severe end-stage manifestation of the disease accompanied by several symptoms including nausea, appetite loss, abdominal tenderness and pain, fatigue and dyspnea, loss of proteins, and electrolyte disorders [15]. Recently, systemic chemotherapy with paclitaxel or S-1 plus cisplatin has improved the treatment of unresectable or recurrent gastric cancer [16–18]; i.p. chemotherapy [19] and immunotherapy, such as with catumaxomab [20], are also encouraging for the treatment of malignant ascites. However, to date, no options have been established for the management of peritoneal dissemination of ascites for patients' refractory to these treatments [15]. In such cases, only palliative therapies, such as paracentesis and diuretics, are available and the prognosis is extremely poor, with a median survival time of 3–4 months [21–23].

Therefore, we undertake adoptive cell therapy by injecting autologous Vγ9Vδ2 T cells expanded ex vivo with zoledronate and IL-2 into the peritoneal cavity of patients with malignant ascites. Direct injection of these cells into the peritoneal cavity allows them access to the tumor cells, bypassing the difficulties of transferred Vγ9Vδ2 T-cell recruitment into solid tumor. Because zoledronate leads to intracellular accumulation of isopentenyl pyrophosphate (IPP)/triphosphoric acid I-adenosine-50-yl ester 3-(3-methylbut-3-enyl) ester (ApppI) in tumor cells that are then recognized by Vγ9Vδ2 T cells by blocking the mevalonate pathway [24, 25], the injection of zoledronate preceded the infusion of expanded Vγ9Vδ2 T-cells (Fig. 1). Using this approach, we asked the crucial question of whether zoledronate-expanded Vγ9Vδ2 T-cells can recognize and kill tumor cells in vivo.

Materials and Methods

Study design and patient selection

This was a one-way, open-label, pilot study in patients with symptomatic malignant ascites secondary to gastric adenocarcinoma requiring symptomatic therapeutic paracentesis. The primary objective of this study was to investigate the safety of i.p. injection of autologous Vγ9Vδ2 T-cells. The secondary objectives were to obtain immunological proof-of-concept of antitumor activity of Vγ9Vδ2 T-cells and to evaluate its clinical benefit. The research protocol was approved by the Ethical Committee of our institution (IRB-ID: P2010019-11Z), and registered at the University Hospital Medical Information Network Clinical Trials Registry (UMIN-CTR) (Unique trial number: UMIN000004130) on August 30, 2010. Written informed consent was obtained from each patient before they entered the study. The study was performed in accordance with the Declaration of Helsinki.

To be included, patients aged ≥20 years had to have histologically or cytologically proven gastric cancer, malignant ascites, an expected survival of at least 3 months, an Eastern Cooperative Oncology Group performance status (PS) of 0–2, normal kidney, liver, and bone marrow function, and be resistant to standard therapies. Patients positive for anti-adult T-cell leukemia-associated antigen or anti-human immunodeficiency virus antibody, other primary cancers, uncontrolled infection, active enterocolitis, severe heart disease, severe drug allergy, cryoglobulinemia, or autoimmune disease, were excluded from the study. Those receiving systemic steroid therapy or who were pregnant or lactating were also excluded. Small-scale 10-day Vγ9Vδ2 T-cell culture screening tests were first performed to establish the reactivity of each patient's Vγ9Vδ2 T cells prior to entry into the study. Proliferation was assessed as Vγ9Vδ2 T-cell count on day 10 of culture/Vγ9Vδ2 T-cell count at the initiation of culture. This value had to exceed 100 for the patient to be included in the study.

When the preliminary test fulfilled the criteria described above, leukapheresis was performed to isolate autologous peripheral blood mononuclear cells (PBMCs) and harvest plasma. Small-scale culture tests and leukapheresis were performed prior to chemotherapy; PBMCs and plasma were cryopreserved and stored before use. Patients received standard chemotherapy first; Vγ9Vδ2 T-cell culture was initiated immediately when patients became resistant to the chemotherapy (Table 1). After 14 days culture, Vγ9Vδ2 T-cells were harvested and administered i.p. to the patient. Four infusions were carried out weekly. The day before Vγ9Vδ2 T-cell injection, patients received 1 mg of zoledronate (Novartis, Basel, Switzerland) (Fig. 1A). To ensure safety, zoledronate was administered intravenously (i.v.) on day 0 and i.p. via a catheter on days 7, 14, and 21 (Fig. 1B). Before each zoledronate or Vγ9Vδ2 T-cell infusion and 1 day after cell infusion, blood (10 mL) was collected and ascites fluid (50 mL) was drained from the peritoneal cavity via the indwelling catheter for immunological analysis. When the

© 2014 The Authors. *Cancer Medicine* published by John Wiley & Sons Ltd.

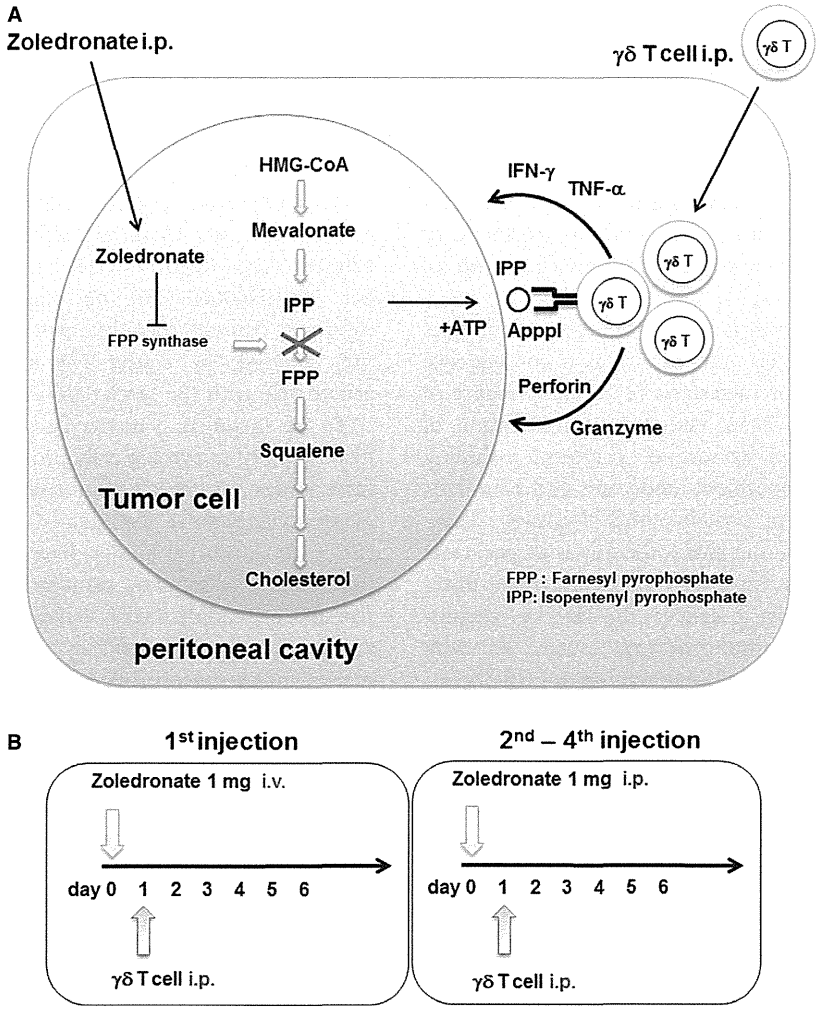

Figure 1. (A) Intraperitoneal administration of zoledronate sensitizes tumor cells to Vγ9Vδ2 T-cell recognition. Isopentenyl pyrophosphate (IPP) is an intermediate metabolite in the mevalonate–cholesterol pathway, recognized by Vγ9Vδ2 T-cells. Zoledronate inhibits farnesyl pyrophosphate (FPP) synthase, thereby causing the accumulation of IPP and triphosphoric acid I-adenosine-50-yl ester 3-(3-methylbut-3-enyl) ester (Apppl) in the tumor cells. When Vγ9Vδ2 T-cells are injected into the peritoneal cavity, they can recognize IPP and respond to tumor cells. (B) The study scheme of weekly i.p. Vγ9Vδ2 T-cell injection. In the first series of injections, zoledronate (1 mg) was administered i.v. on day 0, followed by i.p. Vγ9Vδ2 T-cell injection on day 1. Zoledronate was i.p. injected via a catheter from the second to fourth injection.

patient experienced clinical benefit without significant toxicity, additional Vγ9Vδ2 T-cell infusions were permitted.

Safety assessment, antitumor effects, and quality of life

Medical history, physical examination, PS, vital signs, chest X ray, electrocardiogram, and routine laboratory monitoring (including biochemistry, hematology, urinalysis, and tumor markers) were recorded at baseline. Thereafter, physical examination, PS, vital signs, and routine laboratory monitoring, as well as any adverse events, were assessed at each visit. Abdominal examination was performed by the investigator to assess ascites signs, such as abdominal distension, dullness to percussion, shifting dullness, fluid thrill, and bulging flanks. Subjective symptoms related to ascites, such as anorexia, nausea, vomiting, abdominal pain, abdominal swelling, dyspnea, fatigue, and heartburn, were also recorded. Adverse events were graded according to National Cancer Institute-Common Terminology Criteria for Adverse Events version 4.0. Clinical responses were assessed by computed tomography performed at baseline and after the fourth infusion. To evaluate the antitumor effects of the treatment on peritoneal metastasis, the amount of malignant ascites and peritoneal cytology was also taken into account [26]. Cytology of ascites or peritoneal lavage fluid collected

© 2014 The Authors. *Cancer Medicine* published by John Wiley & Sons Ltd.

Table 1. Summary of patients' background

Patient ID	Age	Gender	Surgery	Chemotherapy
2305	69	F	Exploratory laparotomy	TS-1/CDDP, TS-1/DOC, CPT-11/CDDP, UFT
2307	66	F	Total gastrectomy Roux-en-Y jejunostomy Cholecystectomy Splenectomy	5-FU/MTX, UFT, TS-1/CDDP, DOC
2319	58	F	Bypass surgery	TS-1/CDDP
2325	62	M	Total gastrectomy Roux-en-Y jejunostomy Cholecystectomy	TS-1/CDDP, TS-1/DOC
2334	39	F	Gastroduodenostomy (Billroth I)	DOC, 5-FU+MTX, UFT, TS-1/CDDP
2336	47	F	Bypass surgery	TS-1/CDDP, TS-1/PTX, CPT-11, PTX
2328	55	M	Bypass surgery	TS-1/CDDP, TS-1/DOC

TS-1, tegafur, gimeracil, and oteracil potassium; CDDP, cisplatin; DOC, docetaxel; PTX, paclitaxel; CPT-11, irinotecan; UFT, tegafur-uracil.

through a peritoneal access catheter was carried out using Diff-Quik staining (Sysmex, Hyogo, Japan) according to the manufacturer's instructions. The cellular components of ascites were evaluated using bright field microscopy (OLYMPUS BX41 with a Canon EOS Kiss X4 digital camera, OLYMPUS, Tokyo, Japan, magnification 200×). The safety assessment and clinical responses were determined by an independent data-monitoring committee after completion of the study.

Isolation of PBMC and Vγ9Vδ2 T-cell culture

Vγ9Vδ2 T-cell culture was performed as previously described [10, 27, 28]. For small-scale 10-day Vγ9Vδ2 T-cell culture tests, whole blood (7.5 mL) was collected in BD Vacutainer Cell Preparation Tubes with sodium heparin (Becton-Dickinson, Franklin Lakes, NJ) and directly centrifuged to isolate PBMC. To prepare Vγ9Vδ2 T-cells for the therapy, patients underwent leukapheresis to isolate PBMC and harvest plasma using Fresenius AS.TEC204 with C4Y white blood cell set (FRESENIUS KABI, Bad Homburg, Germany). Sodium citrate (ACD-A solution; TERUMO, Tokyo, Japan) was used as the anticoagulant. PBMC and plasma were isolated by density gradient centrifugation using Lymphoprep (AXIS-SHIELD Poc AS, Oslo, Norway). Leukapheresis yielded more than 1×10^9 PBMC and 100 mL plasma, both of which were cryopreserved until use. Depending on the data from small-scale 10-day Vγ9Vδ2 T-cell culture tests, the number of PBMCs to set up large-scale Vγ9Vδ2 T-cell cultures was estimated in order to obtain more than 1×10^9 Vγ9Vδ2 T-cells for each injection. PBMC were stimulated with 5 μmol/L zoledronate in AlyS203 Vγ9Vδ2 medium (Cell Science and Technology Institute, Sendai, Japan) containing 1000 IU/mL human recombinant IL-2 (Proleukin™; Chiron, Amsterdam, The Netherlands), and 10% autologous plasma. Fresh medium containing IL-2 (1000 IU/mL) was added every 2–3 days and the cultures were transferred into new flasks or culture bags as necessitated by the degree of cell growth. Cultures were split in two to maintain cell density below 1×10^6/mL. Fourteen days after in vitro stimulation, ex vivo expanded Vγ9Vδ2 T cells were harvested and screened for their sterility (negative for endotoxin, bacteria, fungus, and mycoplasma contamination) and purity (>60%). The cytotoxic activity of the Vγ9Vδ2 T-cell cultures was evaluated against zoledronate (5 μmol/L)-pretreated Daudi cells (z-Daudi cells). Those cultured cells which were approved for use after this examination were washed twice with RPMI-1640 and resuspended in normal saline to administer to the patient.

Flow cytometry, immunofluorescence, and cytology

The following monoclonal antibodies (mAbs) were used for flow cytometry: FITC-labeled anti-CD3, -TCRVγ9, and -HLA-ABC, PE-labeled anti-TCR pan αβ, -NKG2D and mouse IgG_1 isotype, PC5-labeled anti-CD3, -CD8, -CD27, -CD56, and mouse IgG_1 isotype, ECD-labeled anti-CD4, -CD45, -CD45RA, and mouse IgG_1 isotype (Beckman Coulter, Immunotech, Marseille, France), PE-labeled anti-CD69 and -TCRVδ2 (BD Bioscience Pharmingen, San Diego, CA), APC-labeled anti-EpCAM (Miltenyi Biotec, Bergisch Gladbach, Germany), and Pacific Blue-labeled anti-CD45 (BioLegend, San Diego, CA). Fixable Viability Dye eFluor 450 and 780 (eBioscience, San Diego, CA) were used to exclude dead cells. The cells were stained with antibodies and analyzed on a Cytomics FC 500 (Beckman Coulter) or Gallios (Beckman Coulter). The data were processed using Kaluza software (Beckman Coulter). Ascites cells were harvested by centrifugation and stained with mAbs described above. Tumor-cell load in ascites fluid (mL) was determined by

© 2014 The Authors. *Cancer Medicine* published by John Wiley & Sons Ltd.

quantification of $EpCAM^+$ tumor cells in ascites fluid/peritoneal lavage. The cells were also resuspended in PBS and examined by confocal microscopy, FV10i (Olympus, Tokyo, Japan).

Cytotoxicity assay

The cytotoxic activity of Vγ9Vδ2 T-cells was examined by flow cytometry as described previously, with minor modifications [11, 29]. Daudi cells were obtained from the RIKEN BRC Cell Bank (Ibaraki, Japan) and grown in RPMI-1640 medium (Wako, Osaka, Japan) containing 10% fetal calf serum, streptomycin (100 μg/mL), and penicillin (100 U/mL). Daudi cells were preincubated with 5 μmol/L zoledronate overnight, resuspended in Diluent C (Sigma, St Louis, MO), and incubated for 2 min with 2 μmol/L freshly prepared PKH-26 (Sigma) at room temperature. Daudi cells without zoledronate pretreatment were also used as target cells. After extensive washing, target cells were coincubated with effector cells at the indicated E/T ratio. After 1.5 h of in vitro incubation, cells in 0.1 mL of binding buffer (10 mmol/L HEPES, 140 mmol/L NaCl, 2 mmol/L $CaCl_2$, pH 7.4) were incubated with 5 μL of Annexin-V-FITC (BD Bioscience Pharmingen) and 20 μg/mL of 7-aminoactinomycin D (7-AAD) (Sigma). Data analysis was performed first by gating on PKH-26-positive target cells followed by the analysis of Annexin-V-FITC- and 7-AAD-positive subpopulations. The percentage cytotoxicity in the PKH-26-gated cell population was calculated by subtracting the value of nonspecific Annexin-V-FITC- or 7-AAD-positive target cells, measured in appropriate controls without effector cells.

$EpCAM^+$ cells were enriched from ascites fluid using CD326 (EpCAM) Tumor Cell Enrichment and Detection Kit, human (Miltenyi Biotec) and stained with PKH-26 (Sigma). The labeled cells were plated on 35-mm glass bottom dish (Matsunami Glass Inc., Osaka, Japan) in RPMI-1640 medium containing 10% fetal calf serum with 5 μmol/L zoledronate. Vγ9Vδ2 T cells from same patient were expanded and labeled with 0.5 μmol/L carboxyfluorescein diacetate succinimidyl ester (CFSE; Molecular Probes, Eugene, Oregon) according to the manufacturer's instructions. After $EpCAM^+$ cells adhered to the bottom of the dish, CFSE-labeled Vγ9Vδ2 T-cells were added and cocultured under the confocal microscopy FV10i observation.

CD107 translocation assay

Daudi cells were preincubated overnight with indicated concentration of zoledronate (0, 1, 5, 10, 50, and 100 μmol/L, Novartis, Basel, Switzerland) to accumulate IPP or 10 μmol/L pravastatin sodium (Cayman Chemical, Ann Arbor, MI) to inhibit IPP synthesis. Zoledronate- or pravastatin-treated Daudi cells were used as stimulator cells and incubated with the same number of Vγ9Vδ2 T-cells (5×10^5) for 2 h at 37°C in the presence of GolgiStop (BD bioscience), and anti-CD107a/b mAbs (BD bioscience). Vγ9Vδ2 T cells were also stimulated with 20 ng/mL PMA/2 μg/mL ionomycin (both from Sigma-Aldrich). Cells were then washed in PBS supplemented with 2% FCS, 1 mmol/L EDTA, and stained for 30 min at 4°C with anti-CD3 and -TCRVγ9. CD107 translocation was measured by flow cytometry.

Cytokine measurement

Cytokines, including IL-1β, IL-2, IL-4, IL-5, IL-6, IL-8, IL-10, IL-12(p70), TNF-α, TNF-β, and IFN-γ in the plasma and ascites fluid were measured using FlowCytomix human Th1/Th2 11-plex kits (Bender MedSystems, Vienna, Austria) according to the manufacturer's instructions.

Results

Patients' characteristics

A total of seven patients underwent adoptive Vγ9Vδ2 T-cell immunotherapy. The characteristics of the enrolled patients are summarized in Table 1. There were two men and five women with a median age of 58 years (range, 39–69). All patients had previously received surgery and chemotherapy. They were resistant to current possible standard chemotherapy, followed by 4-week washout period; then adoptive Vγ9Vδ2 T-cell immunotherapy was reassessed. Malignant lesions were clinically restricted to the peritoneum in two cases (patients 2305 and 2319), while others had metastasized to lymph nodes, ovary, bladder, skin, and bones.

Adoptive transfer of Vγ9Vδ2 T cells

Aliquots of patients' PBMC were thawed and large-scale Vγ9Vδ2 T-cell expansion cultures initiated 14 days prior to each injection. The number and percentage of Vγ9Vδ2 T cells administered differed between individual patients and between separate infusions (Table 2). In most cases, the expansion of Vγ9Vδ2 T cells from cryopreserved PBMCs was successful and $>50 \times 10^8$ Vγ9Vδ2 T cells were prepared for injections. However, the number of harvested Vγ9Vδ2 T cells from the first large-scale culture was less than expected in patients 2305 and 2334, even though the number of cryopreserved PBMCs used was predetermined by the small-scale culture test. In these cases, more cryopreserved PBMCs were used for the next

© 2014 The Authors. *Cancer Medicine* published by John Wiley & Sons Ltd.

large-scale expansion culture to ensure the availability of sufficient amounts of cells. The number of Vγ9Vδ2 Tcells in each injection ranged from 0.6 to 69.8 × 10^8 (median 59.0 × 10^8) (Table 2). The Vγ9Vδ2 T cells from all of the patients displayed good effector function as assessed by their in vitro cytotoxicity against Daudi cells (Table 2).

Activated Vγ9Vδ2 T cells exert antitumor effector activity through TCR and NK receptors such as NKG2D. NK receptors-dependent or Vγ9Vδ2 TCR-dependent recognition of tumor cell was evaluated by CD107 translocation assay using pravastatin- or zoledronate-pretreated Daudi cells (Fig. 2). When the baseline tumor cell recognition by NK receptors was evaluated against pravastatin-treated Daudi cells, %$CD107^+$ Vγ9Vδ2 T cells was 55%. The proportion of $CD107^+$ Vγ9Vδ2 T cells against Daudi or z-Daudi cells increased from 63.3% to 96.9% according to the concentration of zoledronate, and reached the plateau at 50 μmol/L or higher. These results were consistent with previous reports that the optimum inhibition of FPP synthase activity was achieved by high zoledronate concentration [30]. The cytotoxic activities of patients' Vγ9Vδ2 T cells against z-Duadi and Daudi cells were summarized in Table S2.

Dynamics of zoledronate and Vγ9Vδ2 T-cells injection

Three patients completed the course of four Vγ9Vδ2 T-cell transfers; patient 2328 received an additional two

Table 2. Adoptively transferred Vγ9Vδ2 T-cells

Patient ID	Cell number (×10^8 cells) (purity of γδ T cells)				Cumulative number of γδ T cell infusions (×10^8 cells)	Average number of γδ T cell infusions (×10^8 cells)	% cytotoxicity against z-Daudi[1] E/T ratio		
	First	Second	Third	Fourth			1:1	5:1	25:1
2305	0.6 (27.6%)				0.6	0.6	18.1	30.3	30.1
2307	58.8 (81.7%)				58.8	58.8	31.4	40.9	53
2319	55.4 (77.0%)	60.5 (84.0%)	65.6 (85.2%)	68.5 (85.6%)	250	62.5	41.3	58	74.6
2325	49.7 (84.3%)	60 (88.3%)	69.8 (89.5%)	40.1 (89.0%)	219.6	54.9	14.2	39.3	60.2
2334	8.6 (71.5%)	45.1 (77.8%)	52.7 (82.3%)		106.4	35.5	45.1	79.7	84.6
2336	64.9 (94.0%)				64.9	64.9	28.9	57	55.4
2328	62.4 (90.4%)	59.2 (92.5%)	65.7 (93.9%)	51.7 (92.3%)	239	59.8	38.3	64.5	72.2

[1]% cytotoxicity against Daudi cells was provided in Table S2.

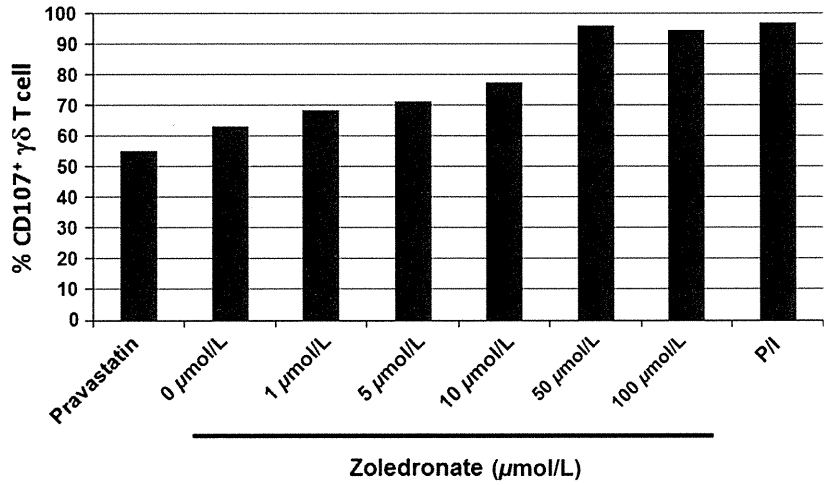

Figure 2. IPP accumulation by zoledronate was evaluated by the CD107 translocation assay of Vγ9Vδ2 T-cells. Daudi cells were preincubated overnight with indicated concentration of zoledronate (0, 1, 5, 10, 50, and 100 μmol/L) or 10 μmol/L pravastatin sodium and used as stimulator cells. The 5 × 10^5 Daudi cells were incubated with the same number of Vγ9Vδ2 T-cells for 2 h at 37°C in the presence of GolgiStop and anti-CD107a/b mAbs. Vγ9Vδ2 T-cells were also stimulated with PMA (20 ng/mL)/ionomycin (2 μg/mL). CD107 translocation was measured by flow cytometry. Results were expressed as percentages of positive cells within the Vγ9Vδ2 T-cell population.

© 2014 The Authors. *Cancer Medicine* published by John Wiley & Sons Ltd.

infusions. After each i.p. injection, a large number of Vγ9Vδ2 T cells was observed in the ascites (Fig. 3A); however, Vγ9Vδ2 T cells were not increased in the blood (data not shown), suggesting that they did not enter the systemic circulation from the peritoneal cavity. The number of Vγ9Vδ2 T-cells in ascites rapidly decreased within 7 days except in patient 2319.

It has been reported that zoledronate declines rapidly from the plasma with half-lives of 0.2 h [31]. By systemic injection of zoledronate, the concentration of zoledronate in the ascites might not be sufficient to block the mevalonate pathway and accumulate IPP in the tumor cells. Therefore, we compared the route of zoledronate injection, i.v. or i.p., preceded the infusion of Vγ9Vδ2 T-cell administration. After i.v. zoledronate and i.p. Vγ9Vδ2 T-cell injection, IFN-γ production was detected in patient 2307 and 2328, but not in patients 2305, 2319, 2325, and 2336 (Fig. 3B). Importantly, the IFN-γ production was observed when both zoledronate and Vγ9Vδ2 T cells were i.p. injected. In patient 2334, i.v. zoledronate injection was omitted; she received three courses of i.p. zoledronate injection followed by i.p. Vγ9Vδ2 T-cell injection. IFN-γ was detected in the ascites with each Vγ9Vδ2 T-cell injection.

Consistently, the concentration of zoledronate in the ascites fluid was higher and sustained longer after i.p. zoledronate injection than i.v. injection (Fig. S1). PBMCs from healthy donor were stimulated with indicated amount of zoledronate in AlyS203 medium containing 1000 IU/mL human recombinant IL-2 and 10% pooled human serum. Same donor derived PBMCs were cultured in IL-2 containing medium and in the presence of 10%

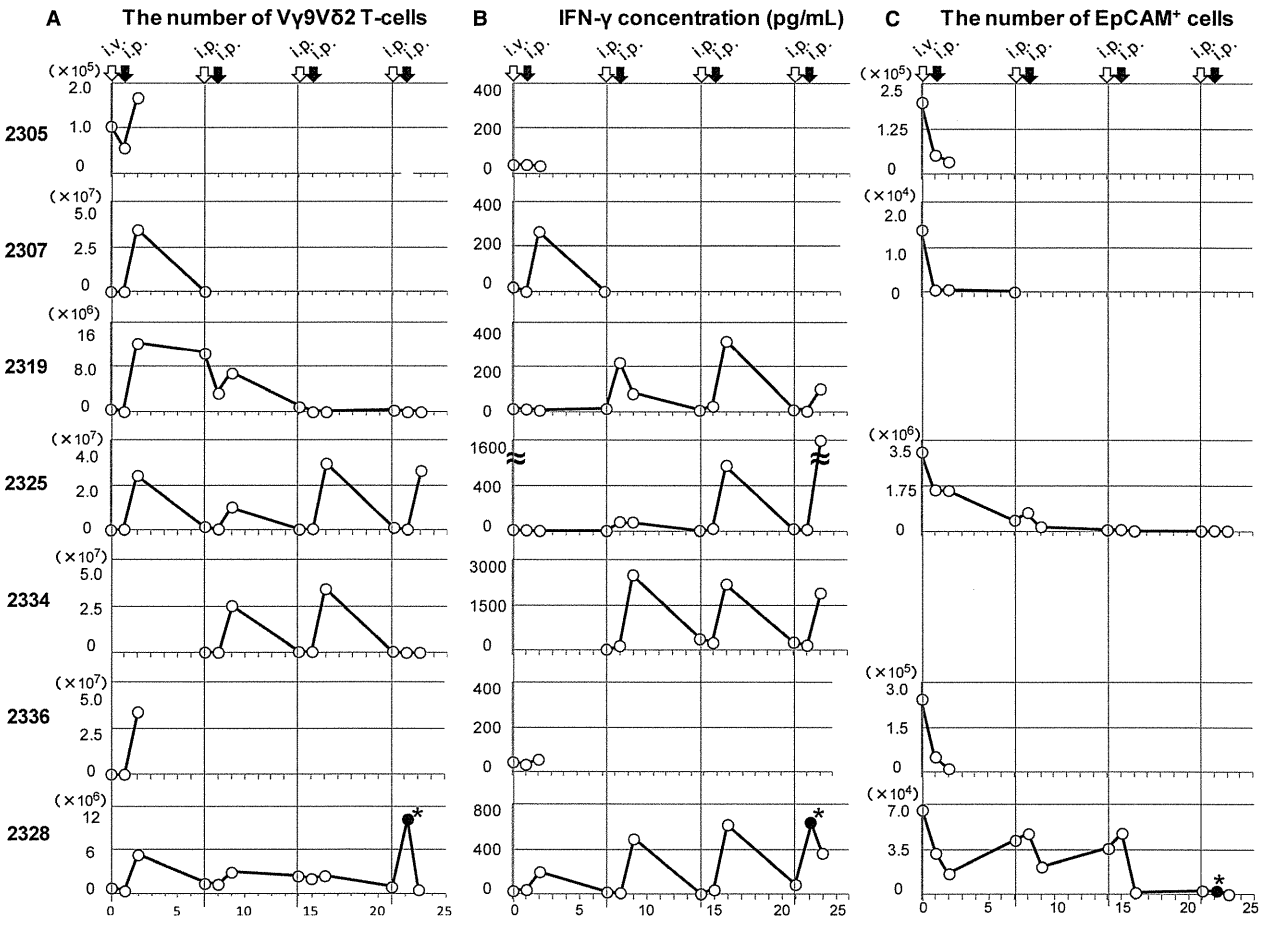

Figure 3. Dynamics of Vγ9Vδ2 T cells and responses in patients with malignant ascites. (A) The number of Vγ9Vδ2 T cells in ascites. The ascites fluid was drained from the peritoneal cavity via the indwelling catheter before zoledronate and Vγ9Vδ2 T-cell injections and 24 h after Vγ9Vδ2 T-cell injections. The cells were isolated by density gradient centrifugation and stained with anti-CD45, -CD3, and -TCRVγ9. The stained cells were analyzed on flow cytometry and the numbers of Vγ9Vδ2 T cells calculated. (B) IFN-γ concentration (pg/mL) in ascites at the indicated time points was measured by the FlowCytomix bead assay. (C) The cells from ascites were also stained with anti-EpCAM mAb and the numbers of EpCAM$^+$ tumor cells calculated. *Sample was collected 4 h after i.p. Vγ9Vδ2 T-cell injection.

© 2014 The Authors. *Cancer Medicine* published by John Wiley & Sons Ltd.